Chapter 1 Introduction

The technology which has become an integral part of modern world has been progressively predicated upon discovering new materials with novel properties. The discovery and application of such new novel materials has tremendous impacts on everyday's life affecting our relationship with data and energy savings, communications, health care and many more. Among such materials, the magnetic materials have immensely fascinated the mankind for many years. In today's life, the magnetism is utilised in many different areas of life including the magnetic memory storage, transformers, television, and read-heads, just to mention some. In the last century, the cassettes and the video tapes were the revolutionary advances of magnetism towards our entertainment whereas today the pen-drives, computer hard disk drives, and credit/debit cards are carrying on the baton of magnetism. However, the increasing needs for the next generation compact, high density memory storage devices and prospects of other applications of magnetic materials drive a new frontier of material research.

1.1 A brief introduction of magnetism

The magnetic property of a system is decided by the spin and orbital motions of its electrons and how the electrons interact with each other (the nucleons also possess magnetic moment but that is negligibly small as compared to the electronic moment). The magnetism of a compound is solely dependent on the electronic configuration of its constituent ions. In case, when all the electrons of an element are in pair, the magnetic spins will cancel each other leading to zero magnetic moment. However, if there exists at least one unpaired electron then the ion will have a net magnetic moment. Different materials behave differently in the presence of an external magnetic field. Therefore, magnetic materials can be broadly divided into several types, viz., diamagnetic, paramagnetic, ferromagnetic, antiferromagnetic and ferrimagnetic. The diamagnetism refers to the weak increase in the magnetization but in the

opposite direction of the applied magnetic field thus it is related to the negative susceptibility. The diamagnetism can be discussed from the classical point of view as: the effect of an applied magnetic field on the orbital motion of an electron raises a back e.m.f. which opposes the magnetic field according to the Lenz's law. However, every material inherently exhibit diamagnetism which is of quantum mechanical origin. In diamagnetic materials, all the electrons remain paired or the orbital shells remain filled, thus giving rise to zero net magnetic moment. On the other hand, the paramagnetic materials show a small but positive susceptibility. In such materials; application of an applied magnetic field induces a magnetization by aligning some of the spins parallel to the applied magnetic field. In contrast to the diamagnetism where the atoms or molecules have no magnetic moment (due to the absence of unpaired electrons) unless an external field was applied, for paramagnetism, the atoms are having a non-zero magnetic moment emanating from the unpaired electrons present. In the absence of an external magnetic field, these spin moments are randomly oriented because the spins on neighbouring atoms interact only very weakly with each other or remains merely independent. The application of an external magnetic field makes them aligned while the degree of alignment or the corresponding induced magnetization depends upon the strength of the applied magnetic field. Two factors control the magnetization in the paramagnetic materials: the strength of the magnetic field and the temperature. Although an increase of the applied magnetic field will tend to align the spins along its direction, the increase of the temperature will result in randomization of these spins due to the thermal fluctuations. The ferromagnetic materials have very strong and positive magnetic susceptibility. They get strongly attracted in external magnetic field. Additionally, ferromagnetic materials have its intrinsic capability to retain its magnetic properties even after the magnetic field is switched to zero. Eventually, the ferromagnetic materials give rise to the formation of the magnetic domains in which the spins remain aligned in a particular

direction. The domain formation is a result of minimization of the free energy of the system. In the normal condition, without magnetic field, the magnetic domains in the ferromagnetic material are organized randomly. However, when we put a ferromagnetic material in the magnetic field, all the magnetic domains in the ferromagnetic material will eventually be parallel in the same direction. Further, when we remove the magnetic field, some domains are still pointing in the same direction thus leading to the remanent magnetization and magnetic hysteresis. In an antiferromagnetic material, there are two magnetic sub-lattices oriented anti-parallel to each other and they are having equal magnetic moments. As a consequence, it has zero net magnetization due to mutual cancellation of the moments. On the contrary, a ferromagnetic material has also two magnetic sublattices aligned anti-parallel to each other similar to the anti-ferromagnetic systems, however, in this case, magnetic moments of one sublattice is larger than the other. This leads to a net magnetization of the ferromagnetic materials. In fact, ferrimagnetic systems exhibit properties of both ferromagnetism and antiferromagnetism.

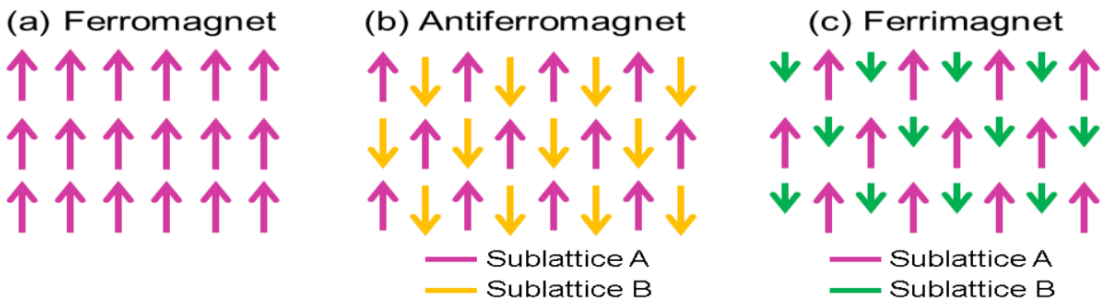

Figure. 1.1: *The spontaneous spin alignments for in a (a) ferromagnet (b) an antiferromagnet (c)a ferrimagnet below a critical temperature called magnetic ordering temperature.*

To demonstrate the microscopic spin structure of the ferromagnet, antiferromagnet and ferrimagnet systems, we have shown it figuratively in Fig. 1.1. All these three magnetic

classes display spontaneous long-range spin ordering beneath a critical temperature (Fig 1.1). The strong magnetic interactions among the spin moments owing to the existence of a large internal molecular field (H_W) give rise to the long range magnetic ordering of such systems. As already mentioned, the spins in a ferromagnet show parallel alignment whereas for both the antiferromagnets and ferrimagnets, nearest neighbour spins display antiparallel alignment. The theory of ferrimagnetism basically uses the concept of two interpenetrating sublattices denoted as sublattice A and sublattice B (as shown in figure) and this theory is factually an extension of Néel's theory of antiferromagnetism. Each sublattice has its own magnetization, M_A and M_B, respectively, which is the product of the composition of each sublattice and its average magnetic moment. The total magnetization can be estimated by taking the difference as $M = |M_A| - |M_B|$. In fact, for an antiferromagnet, sublattice A and B are structurally identical to each other so that $M_A = M_B$, it causes the perfect cancellation of the magnetization leading to zero net moment. For a ferrimagnet, the A and B sublattices are structurally non-identical such that $M_A \neq M_B$. This results in imperfect cancellation of the magnetization and a resultant non-zero net moment for ferrimagnets.

1.2 Spin-frustration

The term frustration in psychology is related to a mental condition of emotion which arises when one typically gets hindrance in achieving a personal goal. The degree of frustration in turn depends on the relative importance of that particular goal. Often, several circumstances of frustration arise from the mental conflict of achieving several goals which require opposing actions. The resulting mental unrest finds its way to manifest itself through unreasonable and passive-hostile actions of the frustrated person. However, when the frustration reaches to a certain critical level, the resulting emotion will try to instigate a path

to solve the problem. Hence, sometimes, a little frustration can lead to some good results if considered in a positive manner.

Interestingly, in magnetism also such frustration among spins occur which manifests in its magnetic properties. The spin frustration can occur in a system which has a specific geometry that hinders it to achieve a particular ground state by minimizing its energy between pairs of interacting spins, this kind of spin frustration is known as geometry driven spin frustration and such systems are known as geometrical spin frustrated systems [1,2]. However, spin frustration can also occur in systems which have randomness or disorder in its magnetic ion sites so that the exchange interactions among the magnetic spins become random, thus on lowering the temperature, the spins attain a random, non-collinear and frozen state instead of a ordered ground state. This kind of spin frustration is known as disorder driven spin frustration. The quenched disorder formed in the lattice during the sample synthesis unintentionally or intentionally (for example; by random substitution of iron atoms in gold matrix) lead to such disorder driven spin frustration.

1.2.1 Geometrical spin frustration

However, the geometrical spin frustrated systems have attracted tremendous research attention world-wide for last few decades as it leads to interesting magnetic properties. In fact, when a system cannot satisfy the simultaneous minimization of all magnetic exchange interactions occurring in the system due the hindrance from its specific lattice geometry, it leads to the macroscopically degenerate numerous low energy states instead of a single ground state [2]. This is indeed analogous to the psychological matter discussed above but here the competing goals are related to the satisfaction of different exchange interactions

(ferromagnetic or antiferromagnetic etc). In this case also, different possible combinations of exchange interactions interfere with each other, hindering the system from reaching its desired situation; where all goals are fulfilled simultaneously. Importantly, a typical feature of geometrically frustrated systems is the lack of long-range spin ordering even at temperatures far below the energy scale of the exchange interactions. Such denial to follow the desired 'directives' can be considered as the magnetic analogy of the “unreasonable and passive-hostile” actions of the frustrated person. Thus, such systems being unable to attain a single ground state typically remain magnetically unordered. This is because of the fact that within the given lattice geometry, the desired ground state for which all the exchange interactions are simultaneously satisfied, does not exist. As a consequence, it reaches a macroscopically degenerate state where a large number of spin configurations are possible having the same, lowest energy states. In principle, although the system may select any one of these lowest-energy states, it actually transforms from one to the other state freely all because of the existence of this degeneracy. These kinds of situations lead to some exotic and special ground states which are exclusively associated to such geometrically frustrated systems, these states include the spin liquid states (where the spins continue fluctuating even at lowest possible temperature), spin ice states (where the spins are constrained to follow the two-in/two out ice rules by the single ion anisotropy) and spin glass states etc [3-11]. However, practically, any smaller perturbations in the system's Hamiltonian which are emanating from exchange anisotropy, crystal field driven single ion anisotropy, interactions with further neighbour, spin-phonon interactions, dipolar interactions, etc can eventually pick up a certain spin configuration leading to the partial lifting of this geometry driven peculiar degeneracy [2]. However, in some cases, by partially lifting this degeneracy (due to the existence of very small energy barriers among the nearly degenerate lowest energy states) the system can develop long-range spin ordering but this partial spin ordering generally takes

place only at the secondary interaction energy scales which is far below that of the individual frustrated exchange interactions. For example, in some geometrically frustrated systems, upon reaching a critical frustration level, the system gives response to the frustrated situation by distorting its lattice at low temperatures showing very strong spin-phonon coupling and ultimately it partially lifts the degeneracy. Eventually, the magnetic properties of such geometrically frustrated systems are mostly decided by these often weak secondary interactions which can largely vary even in the closely similar systems. This is the reason why these different geometrically frustrated systems exhibit interesting and wide spectrum of rich low temperature magnetic states.

To demonstrate the geometry driven spin frustration, we consider a simplest lattice of the form of a tringle as shown in Fig. 1.2. For the exchange interactions between any two spins denoted as *i* and *j*, its Hamiltonian can be expressed as the scalar product of the spin operators as follows:

$$\mathbf{H_{exchange}} = -2J\boldsymbol{S_i}\cdot\boldsymbol{S_j}$$

It is clear from the above expression; the energy is minimized for either parallel or anti-parallel alignments of the spins. In the situation when *J* is negative, giving rise to the antiferromagnetic (anti-parallel) correlation and at the same time *J* is equal for all nearest neighbours (n.n.) pairs, it is clear from the figure that only two of the three spin constrains can be satisfied simultaneously, this brings out the geometrical spin frustration. On the contrary, for the square lattice as shown in Fig.1.2, the spins can satisfy the above conditions therefore can achieve a single ground state, making the system a non-frustrated system.

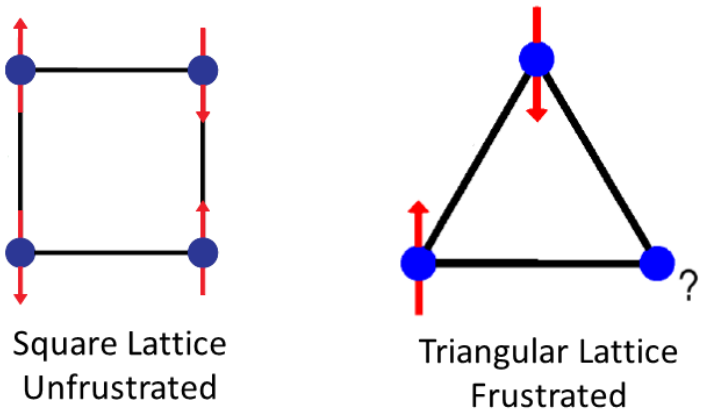

Figure 1.2: *The square lattice satisfies the nearest neighbour AFM interactions (left) while the triangular lattice fails to simultaneously satisfy it.*

However, the example of the geometrical spin frustration in a single triangular lattice can be extended to infinitely extended systems such as hexagonal lattice or Kagome lattice as shown in Fig. 1.3 (a) and Fig. 1.3 (b). It is relevant to mention here that even for a square lattice as well, frustration can be realized if we consider next to nearest neighbour interactions (nnn). However, most of the systems with triangle based lattices exhibit the strong spin frustration. The pyrochlore lattice is basically the three dimensional frustrated lattice. As shown in Fig.1.3 (c), the spins sitting on the corners of a single tetrahedron cannot satisfy the nearest neighbour AFM interactions simultaneously for all the pairs of interacting spins, pair by pair, thus remain frustrated. Thus, the spins (with antiferromagnetic coupling) residing on the vertices of these repeating units (triangles or tetrahedral) of these lattices, there are numerous arrangements of spins with the lowest energy are possible. As these repeating units (triangles or tetrahedra) share maximum of two lattice sites with any of the neighbouring unit (as they are point-shared or edge shared), the whole magnetic system with this structure remains underconstrained and consequently, a macroscopically degenerate states is achieved at very low temperatures, leading to various exotic magnetic phases.

However, it is relevant to mention here that despite of having strong geometrical spin frustration, some of the pyrochlore systems exhibit long range magnetic ordering on reaching low temperatures [2].

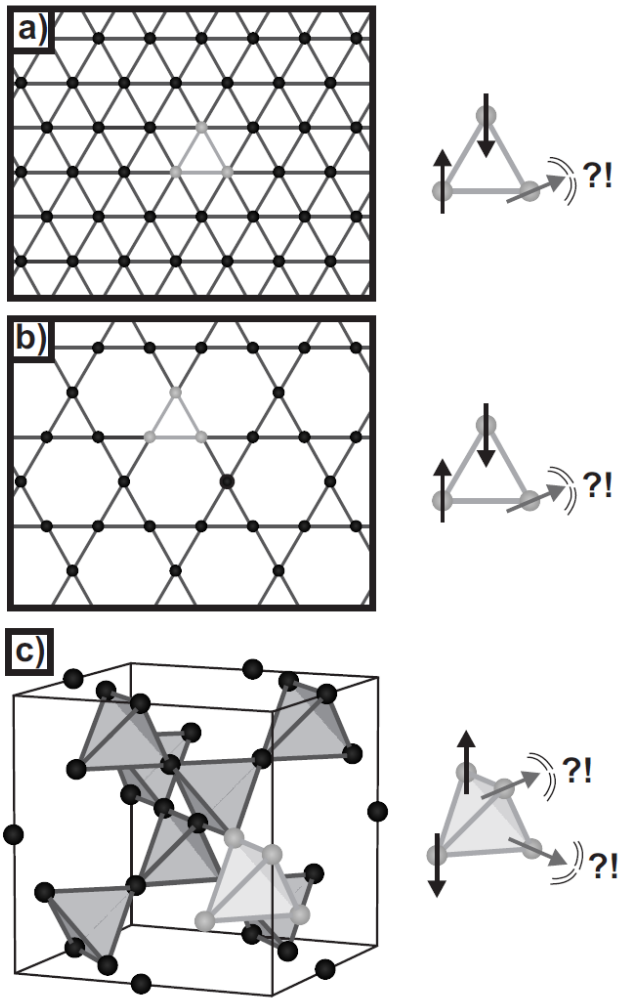

Figure.1.3:*(a), (b) and (c) are depicting a triangular lattice with edge sharing triangles (2D), Kagome lattice of corner sharing triangles (2D) and pyrochlore lattice with corner sharing tetrahedral (3D).*

These long-range ordered states are often triggered by single-ion anisotropy, crystal field effect, further near neighbour exchange interactions, anisotropic spin interactions etc.

Although such systems exhibit long-range spin ordering, these systems are still of considerable interest owing to their magnetization with axial and planar symmetry, quantum mechanical order by disorder effect, partial ordering, highly polarized moments etc [12-16].

1.2.1.1 Crystal structure of pyrochlore oxides:

In fact, the pyrochlore structure is the most common structure which is known to be able to cause geometrical spin frustration. The basic structure of pyrochlore $A_2B_2O_7$ is a derivative of fluorite type (CaF_2) structure which has two cations but one eighth fewer anions (i.e. an unoccupied interstitial site 8a surrounded by four B^{4+} cations). The name "pyrchlore" was originated from the mineral $NaCaNb_2O_6F$, namely pyrochlore [2]. In the year of 1930, Gaertner first reported this structure. The meaning of the name pyrochlore is "green-fire" as upon ignition, it shows green colour. However, the pyrochlore structure is highly ordered as compared to fluorite where site disorder is present. An important parameter which decides the ordering of such $A_2B_2O_7$ structure is the co-ordination number. For, pyrochlore type structure, A (16d) and B (16c) ions are surrounded by 8 and 6 oxygen ions respectively while for fluorite type structure, B ions are prone to be in similar chemical surrounding like A ions (i.e. 8 O^{2-} ions). As the ionic radii of A and B cations come closer, the structure gradually transforms into anion disordered fluorite structure by the migration of some oxygen ions from 48f (O1) and/or 8b(O2) sites to the vacant 8a sites [17,18]. Among different possible families of pyrochlores, $R_2Ti_2O_7$ is a subclass which attracted intense research attention for last few decades owing to its novel and diverse properties. Most of the pyrochlores are cubic in structure with space group symmetry "$Fd\bar{3}m$". At room temperature, almost more than 15 tetravalent ions are there which can sit on the B site of a cubic pyrochlore. In the pyrochlore cubic oxides, the rare-earth elements form a series having the nominal trivalent oxidation state predominantly. Hence, in this series, the ionic radii of A-site ions decrease thoroughly

with increasing atomic number due to the so-called lanthanide contraction effect. However, it is uncommon to observe that the pyrochlore phase shows good stability for all A for a given B. To demonstrate the phase stability of the pyrochlore family most efficiently while displaying the range of stability of pyrochlores with respect to the ionic radii, structure-stability map or the structure-field map as shown in Fig. 1.4 may be considered as was done by Subramanian and Sleight [19]. It is interesting to note here that only B=Sn series can consistently form the stable pyrochlore structures with all rare earth ions. In fact, it is the ratio of the ionic radii i.e. A^{3+}/B^{4+} which determine the phase stability limits for such types of pyrochlore phases. For instance, if the ionic radii of B-site ions be very small (for example Mn^{4+}), a high pressure method must be undertaken for preparing the stable the pyrochlore phases [2]. On the contrary, it is pertinent to note here that $AMnO_3$ type perovskite structure can be easily synthesized in normal air condition without any difficulties. For pyrochlore families, the series with B=V was found to be stable for the first time under ambient oxygen pressure but it was successful only for the three members, Lu, Yb, and Tm with very small ionic radii. However, it was observed that using the high pressure techniques, the series can be further extended [20]. On the other hand, with the Pb^{4+} (the largest) as B ion, it is observed that the smallest rare earth ion for which a stable pyrochlore is formed appears to be Gd. Again, recently, for very small B=Ge ions, stable pyrochlore structure with its typical cubic phase was formed under high pressure otherwise, it remained tetragonal in ambient pressure. Therefore, the range of stability in ambient air pressure can be determined simply by determining the radius ratios: A^{3+}/B^{4+} which lies in between the values 1.36 and 1.71. However, as these limits are approached closer, a marginal stability is expected. Although, some exceptions have also been found, such as, the system $Pr_2Ru_2O_7$ is a stable compound even with radius ratio of ~1.82, but $Pr_2Mo_2O_7$ is not a stable compound even with a smaller radius ratio of ~1.73 [2]. As the radius ratio crosses the critical margin, the site orders both in

terms of the cationic and anionic (oxygen) creep in the structure. Although in such cases, defect pyrcohlores are formed which are also attracting the researchers worldwide for its high ionic conductivity.

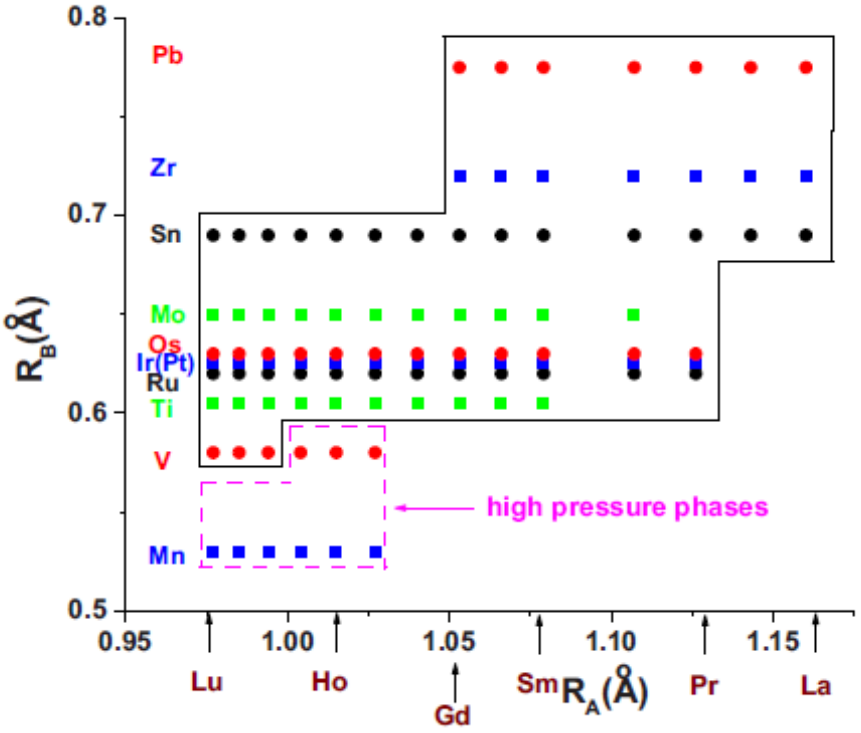

Figure. 1.4: *A stability field or structure field map for showing the stability of pyrochlore materials ($A_2B_2O_7$). (Ref 19)*

1.2.1.2 A brief review of $R_2Ti_2O_7$ (R=rare earth ions) pyrochlore oxides:

●$Dy_2Ti_2O_7$ system:

Among the members of $A_2T_2O_7$ family, $Dy_2Ti_2O_7$ has drawn remarkable research attention owing to its two spin freezing transitions observed at <4 K and at ~16 K [9, 21-24]. In pyrochlore lattice, the frustration occurs usually due to the isotropic Heisenberg exchange interactions for antiferromagnetic coupling among spins. However, it can exhibit frustration even for ferromagnetic interactions when the spins are oriented along an axis joining the

tetrahedron vertices along its centre. For, $Dy_2Ti_2O_7$ the overall spin-spin interactions are of ferromagnetic type but still it is frustrated owing to the crystal field driven single ion anisotropy. Hence, it does not show any long range spin ordering even at lowest available temperatures. Eventually, the normal water ice (ice I_h) is famous for its unusual behaviour. In the common ice, although the oxygen ions develop a periodic stricture but the hydrogen atoms remain largely disordered owing to the existence of two in-equivalent "O–H" bonds in its structure [24]. Pauling had showed by rigorous theoretical calculations that this system should lead to a macroscopically degenerate lowest energy states due to the existence of these two "O-H" bonds. Hence, even when the temperature tends to zero, the system should possess finite entropy. In fact, the dynamics related to this degeneracy are not accessible experimentally as during the melting of ice, the dynamics of hydrogen cannot be investigated independently of oxygen motion. The pyrochlore $Dy_2Ti_2O_7$ is an analogous magnetic system to this common ice, as the degeneracy can be successfully investigated in this system where the orientations of the spins would play the similar roles to that of the hydrogen position in "O-H" bonds [24]. Interestingly, the total spin entropy estimated from the specific heat data of this system $Dy_2Ti_2O_7$ was found to be ~0.67Rln2 which is very close to the value, 0.71Rln2, obtained for common water ice [24]. This undoubtedly established the validity of the correspondence between the two. Hence, $Dy_2Ti_2O_7$ is called as "spin ice" system in which the Dy^{3+} spins are constrained to move like Ising spins along [111] direction. In spin ice materials which follow "ice rules", the rare earth spins are highly uniaxial along <111> direction due to strong crystal field (CF) splitting driven SIA. As a consequence, a highly degenerate macroscopic ground state is observed at very low temperature (<4 K) for all spin ice materials. This happens because any state that follows "two in/two out" ice rule for all the tetrahedra is a ground state which leads to a huge number of degenerate low energy. Under this condition, the system cannot reach an ordered state by minimizing the dipolar

interactions alone and hence ends up in a non-collinear, disordered and frozen state at very low temperature $T<T_{ice}$ ~4 K. Interestingly, of all the spin ice materials $Ho_2Ti_2O_7$, $Dy_2Ti_2O_7$, $Ho_2Sn_2O_7$, $Dy_2Sn_2O_7$ etc.; only $Dy_2Ti_2O_7$ shows a higher temperature spin freezing at 16 K along with its low temperature spin ice freezing at 4 K. This special higher temperature (~16 K) spin freezing for $Dy_2Ti_2O_7$ makes it more interesting towards various research communities and invited intense research attention towards this particular pyrochlore $Dy_2Ti_2O_7$. This 16 K spin freezing is attributed to single ion freezing and it is inter-linked with the low temperature ice freezing (<4 K) by a quantum tunnelling crossover process through the CF barrier and this is explained by creation and propagation of monopoles [21,25].

● $Tb_2Ti_2O_7$ system:

Another member of this $A_2T_2O_7$ family which has also drawn tremendous attention from various research communities world-wide is $Tb_2Ti_2O_7$ [4,5]. This special system is known as a spin-liquid system owing to its persistent spin dynamics down to lowest available temperature. In this system, the Tb^{3+} spins does not show any signs of long range spin ordering down to temperatures below T~ 50 mK [5]. However, it develops nearest neighbour antiferromagnetic interactions below T~50 K which is manifested in the mean field correlation strength estimated from $|\theta_{CW}|$~18 K. This special characteristic of $Tb_2Ti_2O_7$ makes it a cooperative paramagnet or the classical spin liquid such that although its spins are correlated, they keep fluctuating even at T →0 K. The environment of the crystal field (CF) of $Tb_2Ti_2O_7$ is somewhat similar to that of the spin ice systems $Dy_2Ti_2O_7$ and $Ho_2Ti_2O_7$, in which a strong single ion anisotropy along [111] direction has been predicted at T<<20 K. However, unlike the spin ice systems, that has precisely defined Ising type ground-state doublet with its spins directing along the local (111) axis lying more than 200 K beneath its first excited state, the spin liquid $Tb_2Ti_2O_7$ shows a J≈4 ground state doublet along with

another J≈5 crystal field doublet level situating merely above ~20 K in energy. Although, at ambient pressure, no long range magnetic ordering was observed in $Tb_2Ti_2O_7$ but on application of high pressure, it exhibits static long range spin ordering owing to the development of spin-spin antiferromagnetic correlations which co-exist with dynamical states [26]. Apart from that, $Tb_2Ti_2O_7$ also exhibit a field induced unusually slow spin relaxation which is related to the formation of strongly correlated oppositely polarized spin regions, leading to the "single moment saturation"[27]. Moreover, Taniguchi et. al. have investigated the physical properties of $Tb_{2+x}Ti_{2-x}O_{7+y}$ and they have interestingly observed an emergence of long range anti-ferromagnetic state for an unknown accompanying order parameter with a critical value of $x>x_c$ [4]. Hence, this system undergoes a transition from long range ordered state for $x>x_c$ to spin liquid state for $x<x_c$. Moreover, through the detailed temperature dependent Raman spectroscopy study, Mączkaet. al. showed that there exist unusually strong interactions between the crystal field and phonons in $Tb_2Ti_2O_7$ arising due to the spin-liquid state [28].

● $Ho_2Ti_2O_7$ system:

Another interesting pyrochlore system from the same is $Ho_2Ti_2O_7$ which is also known as dipolar spin ice [21, 29-32]. Surprisingly, it does not show the single ion spin freezing transition near ~16 K unlike $Dy_2Ti_2O_7$. The $Ho_2Ti_2O_7$ system behaves as a soft ferromagnetic material owing to the effective ferromagnetic spin-spin correlations with exchange interactions strength of ~1 K among Ho^{3+} spins and hence it shows a positive but small Curie-Weiss temperature ~1.9 K. The local crystal field environment of $Ho_2Ti_2O_7$ is similar to that of $Dy_2Ti_2O_7$ and thus the frustration is emanated by the splitting of the ionic states in the crystalline electric field. For this compound, the single-ion ground state corresponds to merely a pure $|J, M_J\rangle = |8,\pm 8\rangle$ doublet with the separation of ~20.4 meV (~

240 K) from the first excited state [31,32]. Similar to the $Dy_2Ti_2O_7$ system, the spins in $Ho_2Ti_2O_7$ are constrained to point towards the direction of the centre of one of the two tetrahedra (in which it is belonging). It is further observed that through the mutual alignment of two such spins, the system gains energy almost of "two orders of magnitude smaller" than existing the crystal field splitting energy. The estimated dipolar energy (D_{nn}) was found to be ~ +2.4 K [29,30] and the nearest-neighbour exchange interaction energy was found to be (J_{nn}) ~ −0.5 K. Again, similar to the $Dy_2Ti_2O_7$ system, for $Ho_2Ti_2O_7$ system as well, macroscopic ground state degeneracy can be found as this system is also a similar spin ice system obeying the ice rule of 'two in/two out'. As a result, the Ho^{3+} spins also freeze in a non-collinear, randomly disordered fashion below ~1 K. No long range ordering was observed for this system as well down to the temperature: T = 50 mK. As already mentioned, the ~15 K single ion spin freezing transition which is normally visible in $Dy_2Ti_2O_7$ system, is surprisingly absent in $Ho_2Ti_2O_7$. However, later Ehlers et. al. had extensively shown by the neutron spin echo techniques that the 15 K transition is also present in $Ho_2Ti_2O_7$ but it remains masked by the response of the lower temperature spin-ice freezing process [32]. Application of external magnetic field reveals the existence of this transition for this system.

● $Gd_2Ti_2O_7$ system

As already mentioned, antiferromagnetically coupled Heisenberg spins sitting on the vertices of a pyrochlore lattice are supposed to be highly frustrated due to the fact that the exchange energy can be minimized through an infinite number of different paths. The rigorous classical (by Moessner and Chalker) as well as the quantum calculations (by Canals and Lacroix) showed that such pyrochlore system should exhibit a collective paramagnetic state having short-range correlations among its spins at any given nonzero temperature [33-36]. Apart from this, Raju et al. showed that if dipolar spin-spin correlations are considered, it should

lead to an infinite number of degenerate configurations of spins near the mean field transition temperature [15]. Thus, absence of long range ordered state for all the above systems was not surprising. However, later, in their pioneering work, Palmer and Chalker, predicted that a stabilized four-sublattice state is possible to achieve taking the ordering vector k_{ord}=000. Later, the mean field theory calculations showed that a second order magnetic transition (associated to a phase with one disordered and three ordered sublattices) can be possible for such pyrochlore lattice [37]. Moreover, an additional ordered transition was also observed slightly below the temperature of Palmer-Chalker state. On the contrary, a single and highly first order transition to the Palmer-Chalker state was also observed by Monte Carlo simulations. The system $Gd_2Ti_2O_7$ is a special candidate since it contains Gd^{3+} ions with half-filled 4f shell having S=7/2, and L=0, which is considered as the best example of a Heisenberg spin among the rare-earth ions [15]. Interestingly, $Gd_2Ti_2O_7$ was found to enter in a long range ordered state at 0.97 K by ac susceptibility and specific heat measurements. However, later the specific heat investigations further revealed that two different transitions are occurring when magnetic field is applied. The transition with non-zero magnetic field was observed at 0.7 K along with the former transition observed with zero magnetic field at 0.97 K [38, 39].

● $Er_2Ti_2O_7$ system:

Among the members of pyrochlore family $A_2Ti_2O_7$, the Erbium titanate $Er_2Ti_2O_7$ has secured a very special position owing to its exhibition of very strong X-Y (easy-plane) anisotropy so that its local spins are constrained to move in the planes orthogonal to the local <111> axes (i.e. on the planes tangential to the local tetrahedra containing the spins on its corners) [12-14]. The ground state of this system was found to be an insulating antiferromagnet having Curie-Weiss temperature ~-22 K. The crystal field calculations for this X-Y anisotropy yielded an effective moment of ~3 μ_B. Studies by different groups by

neutron diffraction and specific heat etc showed that the system undergoes a continuous phase transition to an unusual non-coplanar structure with long range antiferromegntic ordering, known as ψ_2 state of the Γ_5 irreducible representation [12-14, 40-44]. This particular state of $Er_2Ti_2O_7$ has been explained on the basis of the quantum order by disorder mechanism. In fact, this type of ground state was earlier predicted with a simple nearest neighbour exchange model having the planar anisotropy. In this model, it was shown that this particular state must be selected by "thermal fluctuations" which is described as order-by disorder. It is interesting to note that before the establishment of $Er_2Ti_2O_7$ showing OBD, convincing exhibitions of OBD in real materials were scarce. It is because of the fact that typically the classical degeneracies are not sufficiently symmetry protected to exclude the other weak energetic perturbations which are accountable for stabilizing the long-range order. Recently, an unusual spin dynamics consisting of multiple time-scale relaxations was probed in $Er_2Ti_2O_7$ system [44]. The detailed study of the frequency dependent ac susceptibility unravelled that there exist two distinct spin relaxation mechanisms which are identified as an Orbach process having a pronounced phonon bottleneck effect and cross-tunnelling. The resonant phonon trapping process was attributed to the origin of the observed the phonon bottleneck process.

● $Yb_2Ti_2O_7$ system:

Among the members of the pyrochlore family, $Yb_2Ti_2O_7$ also has placed itself amongst special ones owing to its exhibition of quantum spin ice phase [45-47]. This special state is realized as the condition in which the quantum fluctuations may raise the classical spin liquid state of a spin ice and gradually transform into a complete quantum spin liquid state. In contrast to the normal spin ice systems, quantum spin ice $Yb_2Ti_2O_7$ presents the ferromagnetic exchange combined with X-Y anisotropy. Earlier, specific heat measurement study on this sample showed a sharp singularity around ~0.21 K suggesting a first order

phase transition [46,47]. Later, neutron scattering experiment on the same system eventually revealed an anomaly occurring at the same temperature ~0.21 K where the specific heat peak was observed, thus signalling a magnetic phase transition. The analysis yielded a merely collinear ferromagnetic spin ordering of Yb^{3+} spins having an effective moment of 1.1 μ_B. It also revealed that the spins have slow spin relaxation below transition temperature ~0.21 K. Later, evidence of a Higgs transition from a magnetic Coulomb liquid state to a ferromagnetic state was observed in its single-crystal [45].

● $Sm_2Ti_2O_7$ system

In contrast to the widely studied pyrochlore systems $A_2Ti_2O_7$ with A=Dy, Tb, Gd, Ho, Er and Yb, the $Sm_2Ti_2O_7$ system remained unexplored until a very recent report came up with the observation of a very interesting ordered state with "all in all out" magnetic structure below T_N~0.35 K [48]. The symmetry analysis of the neutron diffraction data of this system yielded that the Ising like Sm^{3+} spins are antiferromagnetically coupled having negligible dipolar interactions and they are forming a "all in all out" structure. In this structure, the adjacent corner shared tetrahedra have alternating all spins directing inwards and all spins pointing outwards as shown in Fig. 1.5. In contrast to the normal ferromagnetic spin-ice state, the "all in all out" state does not lead to the macroscopically degenerate lowest energy states. It is due to the fact that simply placing a single spin as "in" or "out" is sufficient to solely constrain the alignments of all other spins residing on the lattice. However, the study of "Muon spin relaxation" experiment revealed that the spin dynamics persists even at temperatures well below T_N.

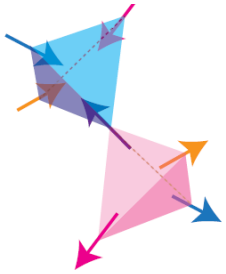

Figure. 1.5: *The all in all out spin configuration in $Sm_2Ti_2O_7$.*

$Eu_2Ti_2O_7$ system:

$Eu_2Ti_2O_7$ pyrochlore system exhibits X-Y like planar spin behaviour due to the presence of strong single ion anisotropy in the system [49]. In the unit cell of $Eu_2Ti_2O_7$, each Eu^{3+} ion is surrounded by 8 oxygen atoms which form a trigonally distorted cube having three-fold inversion D_{3D} symmetry. The interactions between the Eu^{3+} ions and surrounding 8 oxygen ions produce a crystal field with D_{3D} symmetry. The Eu^{3+} spins in $Eu_2Ti_2O_7$ experience strong crystal field effect with D_{3D} symmetry producing different the ionic magnetic susceptibility along and perpendicular to the D_{3d} axis, thus leading to the single ion anisotropy in the system. On the other hand, it is important to note that the strong spin-orbit coupling in Eu^{3+} ions results in forming its electronic pattern consisting of a non-magnetic ground state $^7F_0$ and the first excited magnetic state $^7F_1$lying closely above it. This first magnetic term $^7F_1$ is then followed by other excited magnetic levels $^7F_{2\text{-}6}$lying above $^7F_1$ successively. Again, the crystal field (CF) level splits into further levels e.g. $^7F_1$ splits into a singlet and a doublet. Thus, instead of having a non-magnetic ground state, Eu^{3+} spins show appreciable magnetization. However, the subsequent study on this system by Dasguptaet. al. using the dc magnetization measurements revealed that the dc magnetization of the system $Eu_2Ti_2O_7$ behaves strange below ~68 K reaching a plateau region extending down to ~17 K [50]. This plateau is attributed to the crystal field effect.

1.2.2 Disorder driven spin frustration:

Apart from the geometrical spin frustration, the disorder driven spin frustration is also very important in altering the magnetic behaviour. The disorder driven spin frustration can lead to the formation of the lower temperature re-entrant spin glass or cluster glass states. Griffiths like phase, giant magneto-dielectric coupling, giant exchange bias effects, metamagnetic transition, enhancement of magnetoresistance and magnetocaloric effects etc [51-62]. The disorder can be of different types such as site disorder, chemical disorder or disorder due to the structural distortions etc. The pure long magnetic ordering (viz., ferromagnetic, antiferromagnetic etc) is usually observed in highly structurally ordered systems (exceptions occur for the geometrically frustrated lattices). However, when disorder creeps in the lattice, it raises the random exchange interactions giving rise to the glassy states at lower temperatures where the spins freeze in a random and non-collinear pattern. Eventually, the site disorder in a system has profound effects on its physical properties especially on its magnetic properties altering its magnetic ground state into exotic new states.

1.2.2.1 Double perovskite structure and its properties:

As a matter of fact, the double perovskite systems have offered a fascinating play-ground in both the theoretical and experimental physics for investigating such site-disorder driven novel properties. To understand the structure of double perovskites, we must describe the structure of perovskites. Perovskites take their name from the mineral, which was first discovered in the Ural mountains of Russia by Gustav Rose in 1839 and is named after Russian mineralogist L. A. Perovski.The perovskites structures have the general formula of ABO_3, where A and B are the cations of different sizes (A>B) while O denotes the anions (oxygensetc). The structure is demonstrated in the Fig. 1.6 (a). In its structure, the A cations remain in a 12-fold cubohedral co-ordination while the B cations are in octahedral co-

ordinations of the surrounding anions. In the ideal cubic unit cell of such a structure, the 'A' atom is positioned at cube corner positions (0, 0, 0), the 'B' atom is situated at body-center position (0.5, 0.5, 0.5) and oxygen atoms sit at face centred positions (0.5, 0.5, 0).

The basic unit cell of aordered double perovskitestructure having the formula $A_2BB'O_6$ (A being the rare earth ions, B/B′ are the transition metal ions) is made up of two simple perovskite (i.e. ABO_3 type) basic unit cells with its B and B′ ions alternately placed forming a checker board type pattern as shown in Fig. 1.6 (b).

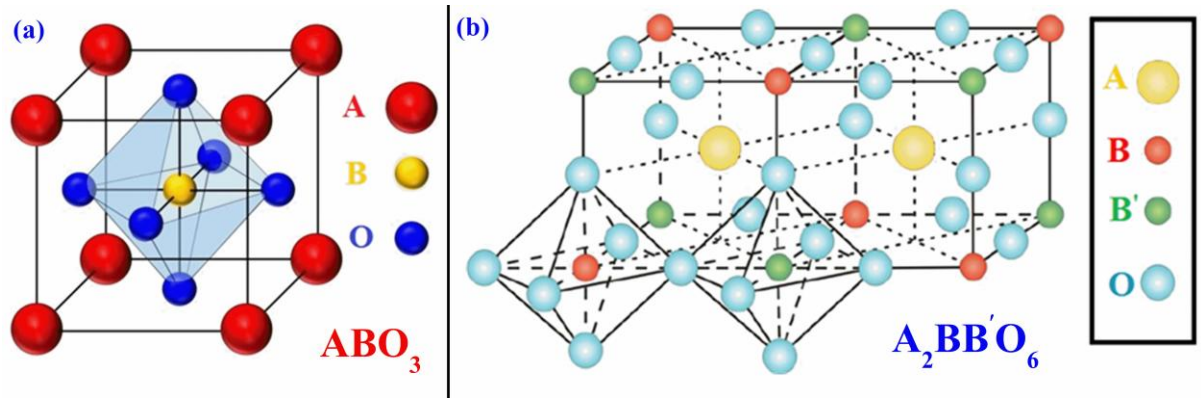

Figure. 1.6: *(a) demonstrates the perovskite structure. (b) depicts the double perovskite structure.*

The novel and unconventional ground states of such DPs are mainly established by the B-site cationic ordering and their nominal valence states. Most of the Co/Ni/Mn based ordered DPs exhibit ferromagnetic (FM) insulating ground state which is best understood by the 180^0 positive super-exchange interactions among B^{2+}/B'^{4+} ions via adjacent oxygen ions following Goodenough-Kanamori rules [57, 63]. As a matter of fact, though a perfectly ordered structure offers a desirable platform for studying its properties theoretically but is extremely difficult to synthesize. The disorders in the form of anti-site disorder (ASD) i.e.

site exchange between B/B' ions inevitably creeps into the structure while sample preparation. Depending upon the B/ B'-site ordering, the DPs are found to crystallize mainly into two types of structures: (1) the ordered monoclinic structure with P_{21}/n symmetry (2) the B-site disordered orthorhombic structure with Pnma symmetry [64,65]. Again, the self-ordering of the B/B' site ions in ordered DP occurs when these two ions have significant difference in their ionic radii and the charge states. Conversely, B-site disorder occurs for same charge states of B-site ions. Additionally, introduction of B^{3+}/B'^{3+} ions as a disorder leads to competing anti-ferromagnetic (AFM) interactions in the system. However, despite the intense research interests and meticulous investigations on such DPs, complete understanding of its electronic structure is still far from well understood.

1.2.2.2 A brief literature survey on R_2BMnO_6 (B=Co/Ni) systems:

● La_2CoMnO_6 system:

The double perovskite La_2CoMnO_6 is amongst the most attractive materials owing to their fascinating properties and potential on practical applications [57, 66-77]. This system in its ordered form is a ferromagnetic insulator with magnetic ordering temperature T_c~225 K. It was also observed that the partially disordered La_2CoMnO_6 system shows two ferromagnetic transitions corresponding to the ordered phase Co^{2+}-O^{2-}-Mn^{4+} showing transition at a relatively higher temperature~210 K and the disordered phase contributes through Co^{3+}-O^{2-}-Mn^{3+} interactions showing the transitions at ~150 K. This system shows a wide variety of properties. The system was reported to show large magneto-caloric effect [73,74]. The strong interplay of its phononic and spin degrees of freedom was also observed in this system [75]. The system intrinsically showed the strong magneto-dielectric behaviour as well which was reported to be highly influenced by its anti-site disorder effect [69]. Apart from this, the magneto-dielectric effect observed in this system might be originated from the spin-phonon

coupling present in the system. Also the system is reported to exhibit reasonably good thermo-electric properties [72]. The nano-particles of this system also showed a prominent cluster glass state around ~38 K which is again attributed to its inherent anti-site disorder [68]. A colossal magneto-resistance effect (~80%) was also observed in this system [76]. The large magneto-dielectric effect was observed in its thin films as well. Again, further works by heterovalent Sr doping in La site of La_2CoMnO_6 lead to the observation of giant spontaneous (H_C~0.65 T) as well as giant conventional (H_C~1.17 T) exchange bias effects [77].

● **La_2NiMnO_6 systems:**

The double perovskite system La_2NiMnO_6 has attracted immense research attention world-wide and thus it is an extensively studied system [52, 54, 78-80]. The highly ordered La_2NiMnO_6 system shows a ferromagnetic transition at ~270 K and it is an insulator in nature [52]. However, such ordered La_2NiMnO_6 system did not show any other transitions at lower temperatures. On the other hand, partially ordered La_2NiMnO_6 system is reported to exhibit an additional glassy transitions below 150 K this is again ascribed to the anti-site disorder driven state [54]. Both the ordered and disordered La_2NiMnO_6 systems show the magneto-dielectric couplings. Interestingly, the magneto-dielectric effect suddenly vanishes below~210 K for the perfectly ordered La_2NiMnO_6 system while its partially disordered one exhibits substantial magneto-dielectric effect even down to 150 K. Most interestingly, it shows the magneto-dielectric effect even at room temperature and the value is very high (~16%). Recently, in the thin film of La_2NiMnO_6, appreciable ferroelectricity was observed [80]. The lattice distortion associated with the A-site displacements is believed to stabilize this ferroelectric polar state in this strained system. The bulk as well as the thin films of this compound is reported to exhibit strong spin-phonon coupling [64]. Moreover, the system also shows near room temperature giant magneto-resistance effect [79]. Later, it was observed that the magnetic field dependent magneto-resistance curves show two distinct regions i.e. the

low-field magneto-resistance which exhibits a sharp rise in an external magnetic field within 200 Oe while the high-field magneto-resistance shows a slower rise with the applied magnetic field (>200 Oe) [79]. Eventually, the low-field magneto-resistance behaviour was explained on the basis of the increased electron tunnelling probability which is accompanied by the orientation of ferromagnetic domains under external field. On the other hand, the high-field magneto-resistance was elucidated by the decreased scattering from the spin defects emanating from the Ni/Mn antisite disorders. It also shows relaxor like dielectric behaviour with very high dielectric constant. Interestingly, study by the electron spin resonance spectra on this system surprisingly revealed that even above the ferromagnetic ordering transition (~270 K), the system does not behave purely as a paramagnet. It revealed that a purely paramagnetic state exists only above the temperature ~ 390 K and the behaviours of the spectra were well explained through the small polaron hopping model. In between these temperatures (270 K<T<390 K), the system develops some short-range magnetic ordering related to the magnetic polarons. Furthermore, the system also showed reasonable amount of exchange bias effect which was effectively tuned by the Sr doping [78]. Moreover, a metal-insulator transition was observed by Sr doping in this system.

● **Y_2CoMnO_6 system:**

Another member of the double perovskite family which attracted considerable research attention is Y_2CoMnO_6 mainly due its exhibition of E-type of spin ordering driven ferroelectricity and the meta-magnetism [81-85]. Interestingly, in this compound, the rise of the ferroelectric polarization is believed to be driven by the special E-type of magnetic structure (↑↑↓↓) of the spin chain Co^{2+}-Mn^{4+}-Co^{2+}-Mn^{4+} which causes the magnetostriction effect leading to the observed ferroelectricity [83]. Apart from this, this system exhibits unusual meta-magnetic transition in the form of very sharp steps in the isothermal magnetization curves [81,83]. This feature is very unique to this system and elucidated by the

presence of anti-phase boundary arising through the inherent anti-site disorder of the system. However, the later study on this compound extensively showed the roles of the anti-site disorder in manifesting its magnetic properties. They have also explained the origin of the ferroelectricity observed in this system by means of the extrinsic effects like trapped charges, defect dipoles etc instead of the E-type of magnetic ordering [53]. Their study showed that no super-lattice magnetic reflection peak was observed owing to the E-type of magnetic ordering. On the other hand, Y_2CoMnO_6 also showed a very interesting and rare property by showing the simultaneous exhibition of the electro-caloric effect as well as the magneto-caloric effect at the ferroic ordering temperature ~75 K [85]. Thus the observation of such multi-caloric effect in this system placed this amongst the very rare materials. Moreover, a recent study revealed its interesting property related to the spin-lattice interactions. Eventually, the system showed prominent spin-phonon coupling for at least two phonon-modes which is very rare and highly interesting.

● **Y_2NiMnO_6 system:**

The compound Y_2NiMnO_6 has also attracted considerable research attention for last few years [86-90]. The theoretical ab initio study on this structure predicted an anti-ferromagnetic E-type of magnetic structure (↑↑↓↓) with Ni^{2+}/Mn^{4+} spins similar to the Ca_3CoMnO_6 spin chain [86]. This special magnetic spin structure is further predicted to produce sizeable ferroelectric polarization by breaking the inversion symmetry. Hence, to some extent, this system is believed to be similar to Y_2CoMnO_6 system. However, as already stated, no experimental evidence of E-type of magnetic ordering has been observed in Y_2CoMnO_6. Later, Su et. al. have experimentally shown the emergence of the ferroelectric polarization which was explained on the basis of the E-type of magnetic spin structure and the charge ordering of Ni^{2+}/Mn^{4+} ions [88]. The nano-crystal of this compound showed the multiferroic properties by showing the ferromagnetic property (T_C~92 K) as well as higher

temperature ferroelectric transition (~535 K). Again, similar to the Y_2CoMnO_6 case, in Y_2NiMnO_6 compound as well, the origin of the ferroelectric polarization has been shown to be arising from the re-orientation of the electric dipoles raised from the free-charges (rather than the magnetic structure driven ferroelectricity) [90]. Thus, the prediction of the E-type of magnetic ordering has been ruled out. Apart from this, the temperature dependent Raman spectroscopy study of this system also revealed the existence of strong spin-phonon coupling [87].

● **Lu_2CoMnO_6 system:**

The system Lu_2CoMnO_6 has also received invigorated research interest globally owing to its magnetic-structure driven ferroelectricity [91-94]. The study on its single crystal revealed that there exists strong coupling between the ferroelectric and magnetic properties in this system [92]. In this system, the collinear magnetic ordering of the Co-Mn-Co-Mn chains in ↑↑↓↓ fashion breaks the spatial inversion symmetry leading to the creation of the electric polarization in this system. In this system, below the temperature ~43 K, a magnetic transition takes place and a ↑↑↓↓ type of magnetic spin ordering sets in the system whereas the ferroelectric transition takes place below~35 K. On the contrary to the earlier two systems Y_2CoMnO_6 and Y_2NiMnO_6, the ↑↑↓↓ type spin structure has been experimentally observed in Lu_2CoMnO_6 by neutron diffraction study [91]. To explain the above phenomenon of magnetism driven ferroelectricity in this system, the concept of the "domain boundary" which refers to the boundary between ↑↑ and ↓↓ spins along the c axis of the crystal. Due to the presence of two different kinds of ions in this system (Co^{2+}/Mn^{4+}), two types of domain walls are also present: the one which is centred on Co^{2+}-Mn^{4+} bonds while the other is centred on Mn^{4+}-Co^{2+} bonds. As a result, these different domain walls also have opposite electric polarizations since their way of breaking the local spatial-inversion symmetry is exactly opposite. So it can be understood as: the domains walls of these ferromagnetically

aligned spins bear an internal degree of freedom of electric polarization arising from the small structural distortions formed due to the magnetostriction effects caused by the domain walls. This in turn causes the coupling between the magnetic and electric degrees of freedom [93]. Eventually, a perfectly aligned ↑↑↓↓ spin structure can be considered as a condensation of domain walls whose electric polarizations are all aligned. If in the presence of an electric field, the sample is cooled through its transition temperature, it would essentially store a net electric polarization by inducing more domains walls with one polarization than with the opposite. As a matter of fact, this electric polarization can be mostly destroyed by applying high magnetic field of ~1.5 T. However, an additional small electric polarization still persists up to magnetic field of 60 T [92]. However, the ferroelectric polarization arises along c axis in such polycrystalline system. Interestingly, in its single crystal, the ferroelectric polarization was observed along the b-axis instead of c axis. Since, the magnetic control of the ferroelectricity is quite precise in this system, it has potential to be used in practical applications like memory storage. Later, Zhou et. al. had theoretically showed by first principle calculations that the electric polarization should occur along b axis indeed instead of the c axis of this system with $P2_1/n$ symmetry [93]. Later, Zhang et. al. came up with an interesting results by first principle calculations regarding the spin structure driven ferroelectricity in this system [94]. They have extensively shown by calculations that the system has a ferromagnetic ground state instead of the antiferromagnetic ↑↑↓↓ type spin structure. However, though the ground state is inclined to lead to the ferromagnetic ordering, the presence of the weak out-of-plane nearest neighbour exchange interactions along with the exchange-striction effect eventually lead to the very close energy difference between the ferromagnetic and the ↑↑↓↓ spin structures. As a consequence, in the real systems, where the anti-site disorder is unavoidable, the resulting antiferromagnetic exchange interactions can essentially balance this small energy difference, thereby leading to the formation of ↑↑↓↓ spin

structure. This spin structure then leads to the ferroelectricity in the system. However, they had ruled out the role of the charge ordering in the observation of the ferroelectricity. The E-type of Co/Mn spin structure in this system is demonstrated in the Fig. 1.7.

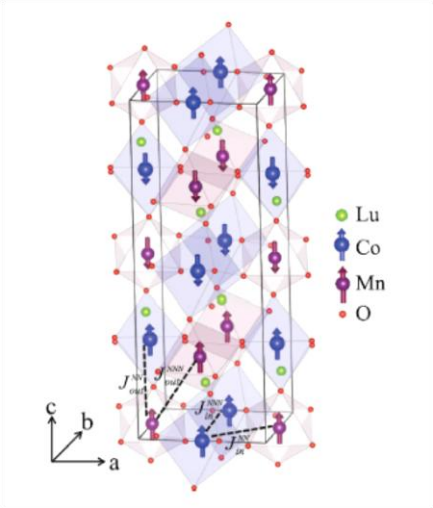

Figure. 1.7: The E-type of Co/Mn spin ordering in Lu_2CoMnO_6. (*Zhang et. al., Phys. Rev. B 93, 075140 (2016)*)

● **Lu_2NiMnO_6 system:**

The system Lu_2NiMnO_6 is relatively less studied system [95,96]. It orders ferromagnetically at~45 K and it is an insulator. It also shows colossal value of the dielectric constant as well as small negative magneto-dielectric effect [95]. Moreover, this system has exhibited magnetocaloric effect as well [96].

● **Pr_2CoMnO_6 system:**

The double perovskitePr_2CoMnO_6 is also an interesting system as it shows a broad range of properties including the Griffiths like phase, exchange bias, magneto-dielectric effect and spin-phonon coupling [97]. It is also a ferromagnetic insulator in nature. However, no comprehensive study of its electronic structure as well as the spin dynamics is available in literature to date. Hence, further study by neutron diffraction, ac susceptibility measurements

and electronic structure by different spectroscopic techniques may explore the intriguing physics behind its interesting magnetic properties.

● **Pr_2NiMnO_6 system:**

The candidate Pr_2NiMnO_6 also is an ferromagnetic insulator which crystallizes in ordered monoclinic phase with $P2_1/n$ symmetry [98,99]. This system is reported to show weak spin-phonon coupling in the stretching vibrational phonon mode.

● **Dy_2CoMnO_6 system:**

The system Dy_2CoMnO_6 shows similar properties to the other ordered double perovskites systems [100]. It also crystallizes in $P2_1/n$ monoclinic structure. It shows two magnetic transitions at ~85 K which is related to the ferromagnetic transition due to the ordering of the Co/Mn sublattice. It is also reported that this particular compound shows metamagnetic transition as well as appreciable magneto-caloric effect.

● **Dy_2NiMnO_6 system:**

The compound Dy_2NiMnO_6 shows two magnetic transitions at 100 K owing to the magnetic ordering of the Co/Mn spins while the lower temperature transition observed at ~20 K is related to the Dy ordering [101]. It showed magnetodielectric effect near the Dy ordering temperature, hence it is intrinsically related to the Dy ordering.

● **Sm_2CoMnO_6 system:**

The system Sm_2CoMnO_6 is also a ferromagnetic insulator having its magnetic transition temperature at ~135 K [102]. For this compound as well, the proposed spin structure is up-up-down-down, however, it is yet to be confirmed. It shows metamagnetic transition from an antiferromagnetic state to a spiral magnetic state. It is also reported that this system exhibits ferroelectric polarization which is intrinsically driven by the magnetic ordering. The

metamagnetic transition was observed to alter the electric polarization significantly. Furthermore, Ca doping in the Sm site was observed to drive the system into a phase separated system [103]. It was also observed that the Ca doping raised very high exchange bias in the system.

● **Sm_2NiMnO_6 system:**

Similar to the other double perovskite compounds, $Sm_2NiMnO_6$is also a ferromagnetic insulator having a ferromagnetic transition at ~156 K [104, 105]. However, on lowering the temperature, this system enters in a re-entrant spin glass like state. Moreover, it shows very interesting magneto-dielectric coupling effects by exhibiting both the positive and negative magneto-dielectric effects. Above the magnetic transition temperature, it is reported to show extrinsic colossal magneto-dielectric effect while it showed positive intrinsic magneto-dielectric effect below the magnetic transition temperature [105].

● **Nd_2CoMnO_6 system:**

The system Nd_2CoMnO_6 has received renewed interest owing to its diverse interesting properties [106-109]. It showed ferromagnetic transition around~150 K in its bulk form. On the contrary, its epitaxial thin film showed the ferromagnetic transition around~175 K as well as a ferroelectric transition at ~585 K [107]. It also showed magneto-dielectric coupling effect near its ferromagnetic transition ~175 K. On the other hand, its thin film formed under biaxial strain exhibited significant spin-phonon coupling effect [109]. Additionally, this compound is reported to show very large ferroelectric polarization ~1.3 $\mu C/cm^2$ which is much higher than the polarization observed in other similar systems [106]. The polarization is seemingly associated to the ↑↑↓↓ spin structure which is in turn related to the anti-site disorder driven anti-ferromagnetic exchange interactions. Recently, another study on this

compound revealed that this system exhibits a re-entrant cluster glass state around~135 K as well as meta-magnetic transition at low temperatures [108].

● **Nd_2NiMnO_6 system:**

The compound Nd_2NiMnO_6 is also a ferromagnetic insulator like other members of double perovskite [110-113]. However, it is reported to show two ferromagnetic transitions at ~193 K and ~105 K owing to the magnetic super-exchange interactions Co^{2+}-O-Mn^{4+} (from the B-site ordered ions) and Co^{3+}-O-Mn^{3+} (coming from the B-site disordered ions) [112]. In another report on the same compound, it is reported that the system undergoes a re-entrant cluster glass transition owing to the anti-site disorder present in the system [110]. Moreover, the exhibition of exchange bias effect by this compound was also reported at low temperatures [111]. Later, the study on its epitaxial thin film also revealed its exhibition of spin glass and exchange bias effect [113].

● **Gd_2CoMnO_6 system:**

The system Gd_2CoMnO_6 has also received the considerable research interest world-wide for its exhibition of wide range of interesting magnetic properties [114-119]. Initially, Wang et. al. reported this system to exhibit a spin glass like transition around 112 K followed by an antiferromagnetic transition around ~43 K [114]. However, later, studies by many groups have identified this 112 K transition to be a ferromagnetic transition instead of the spin glass like transition [115-119]. However, below 50 K, the short range ordering of the Gd^{3+} ions starts due to 3d-4f negative exchange interactions and it starts dominating over the Co/Mn ordering below 20 K [116,117]. This particular candidate has received much attention because of its superior magneto-caloric properties than any other members of its family [115,116]. Moreover, Hopkinson's peak had been identified in the ac susceptibility study of this compound which is attributed to the competing "antiferromagnetic and ferromagnetic" interactions along with the strong anisotropy field [117]. An enhanced magneto-caloric effect

was observed with the Sr substitution in the Gd site through an effective increase in the ferromagnetic ordering [118]. Giant value of the magneto-caloric effect was also observed in the single crystal of Gd_2CoMnO_6 compound [115]. Moreover, a weak spin-phonon coupling was also observed in the same system in its polycrystalline form [119].

● **Gd_2NiMnO_6 system:**

The compound Gd_2NiMnO_6 is a ferromagnetic insulator with the ferromagnetic ordering temperature ~134 K [120]. An additional magnetic ordering also occurs by Gd^{3+} spins at around ~33 K. Interestingly, this system shows a Griffiths like phase above the ferromagnetic ordering temperature extending up to 230 K. Also, this system also showed magneto-dielectric coupling. Moreover, the magneto-caloric effect as well as the spin-phonon coupling was also reported in this system [121].

● **Tb_2CoMnO_6 system:**

The system Tb_2CoMnO_6 is a ferromagnet with ordering temperature ~98 K [122-124]. However, at lower temperature, it enters in a glassy region owing to the competition between the ferromagnetic positive superexchange interactions between Co^{2+}-O^{2-}- Mn^{4+} and the negative antiferromagnetic interactions of Co^{2+}-$O^{2-}$$Co^{2+}$ and Mn^{4+}-O^{2-}- Mn^{4+} [122]. It also exhibits sharp metamagnetic transition. It is also recently reported that this compound exhibits giant rotational magneto-caloric effect ~20.8 J/kg K at 2 K [124].

● **Tb_2NiMnO_6 system:**

This particular compound Tb_2NiMnO_6 is also a ferromagnetic insulator which crystallizes in $P2_1/n$ monoclinic phase [125]. The magnetic ordering occurs at ~111 K. Among the very few compounds of the double perovskite family, this particular system shows clear Griffiths like phase above the paramagnetic transition temperature. Moreover, it also exhibits weak spin-phonon coupling below the magnetic ordering temperature.

● **Er_2CoMnO_6 system:**

The compound Er_2CoMnO_6 remained unexplored for long time, until Banerjee et. al. investigated its properties [126]. The system shows very interesting properties including the ferromagnetic ordering at low temperature, inverse exchange bias effect and strong magneto-dielectric effect. In fact, the inverse exchange bias effect is very scarce in materials. The system also shows the magnetization reversal effect and the spin compensation effect, the underlying physics of which involves the existence of the three different magnetic ions, specially the 4f Er^{3+} ions which has the larger uniaxial anisotropy. The origin of the inverse exchange bias is seemingly associated to the negative exchange interactions occurring at the interface of the ordered and disordered (due to the anti-site disorder) magnetic phases. Very recently, another report on this compound revealed that it shows strong magneto-dielectric coupling as well [127].

1.3 Some important physical phenomena related to our research:

1.3.1 Crystal Field Theory:

The crystal field theory is based on an ionic model and it neglects covalent bonding character. The theory essentially provides a qualitative description of some special features of the transition metal oxides.

Let us consider an isolated $3d^n$ transition metal cation as shown in Fig. 1.8. The energy levels related to its d orbitals are five-fold degenerate in nature. However, when placed in a crystal field, the 3d valence electrons will face the electrostatic field produced by the oxygen ligands. As a consequence, the energy is enhanced due to the coulombic repulsion between the valence electrons of the cation and surrounding ligands. The reduced symmetry finds that

the energy of the system is diminished by lifting the five-fold degeneracy of the d orbitals and as a result, it split them into two energy levels: a triply degenerate level consisting of the d_{xy}, d_{yz} and d_{xz} orbitals (these are known as t_{2g} level) and a doubly degenerate level consisting of the d_{z^2} and $d_{x^2-y^2}$ orbitals (known as e_g level). Interestingly, the symmetry of the crystal field essentially alters the relative positions of these energy levels [129]. It can be realized for the octahedral and tetrahedral symmetries by visualizing the orientation of the d orbitals together with their oxygen ligands. The transition metal ion is surrounded by six nearest neighbour ligands in an octahedral co-ordination. In such coordination, Fig. 1.8 demonstrate that the d orbitals split into lower energy t_{2g} orbitals and higher energy e_g orbitals adopting the electronic configuration $(t_{2g})^m(e_g)^n$ where m and n are integers and t_{2g} and e_g are group symmetry notation.

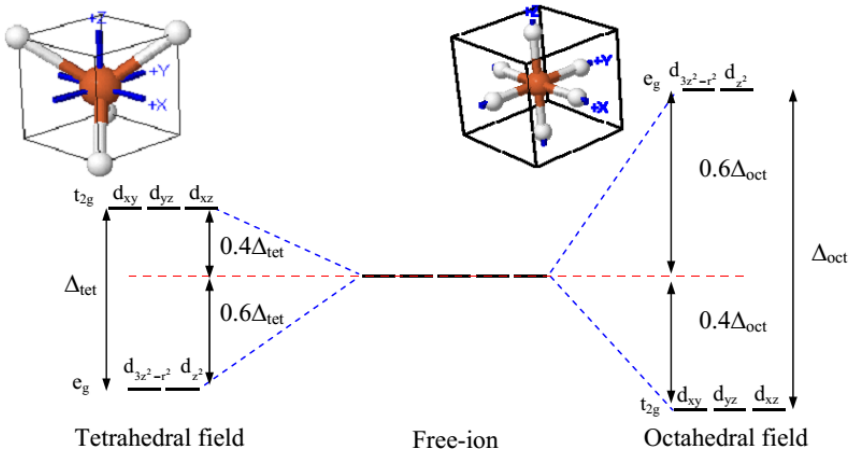

Figure. 1.8: *The energy levels of the orbital in the d-electron system. The energy levels split into t_{2g} and e_g where these levels are inverted for both fields also the energy gap in the tetrahedral field is smaller than the energy gap in the octahedral field (from reference [128])*

The positions of the oxygen ligands (treating them as point charges) are shown in Fig. 1.9. As a matter of fact, the crystal field is the highest for the e_g orbitals as these are directly pointing towards the ligands: d_{z^2}points towards the z axis while $d_{x^2-y^2}$ points towards the x and y axes. On the other hand, the t_{2g} orbitals i.e. d_{xy}, d_{yz}, and d_{xz} do not point along the coordinate axes instead they point in between them where the field is weaker. Eventually, the stronger crystal field effects in e_g orbitals creates larger electrostatic repulsion between the electrons of the e_g orbitals and ligands. This results in raising their potential energy (e_g) and makes them energetically less stable compared to the t_{2g} orbitals which have lower energy. On the contrary, in the tetrahedral co-ordination, a cation is surrounded by four ligands (anions). In this case as well, the crystal field splits the five-fold degenerate d orbitals into triply and doubly degenerate energy levels as shown in Fig. 1.9.

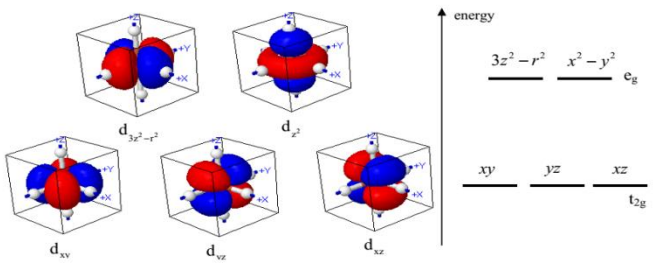

Figure.1.9: *The orbitals of tetrahedral field, the energy levels split into triply degenerate t_{2g} and doubly degenerate eg where the energy level of t_{2g} orbitals is higher than the energy level of e_g orbitals (from reference [128]).*

Interestingly, the relative positions of these energy levels are opposite to the former case. Here, the d orbitals are split into lower energy e_g orbitals and higher energy t_{2g} orbitals adopting the electronic configuration $(e_g)^p(t_{2g})^q$ where p and q are integers. It can be seen from the Fig. 1.10 that the t_{2g} orbitals are in closer proximity to the ligands which point

towards the midpoint of the cube edges than the e_g orbitals which point along the center of the cube faces. Similar to the previous descriptions about the octahedral crystal field, the greater coulombic repulsion between the electrons of the t_{2g} orbitals and ligands leads to their higher energy compared to the e_g orbitals. In fact, no d orbital lobes point directly at the ligands for the case of the tetrahedral symmetry. The crystal field splitting (Δ) i.e. the splitting between the t_{2g}/e_g levels differs in value for octahedral (Δ_o) and tetrahedral (Δ_t) symmetry. As evident from the Fig. 1.9, $\Delta_t<\Delta_o$ and the analysis have yielded the value of Δ_t/Δ_o ratio ~ 4/9[130]. This can be understood as in tetrahedral symmetry, the d orbitals point along the directions where the crystal field is even less than that of the octahedral t_{2g} orbitals leading to a smaller crystal field splitting.

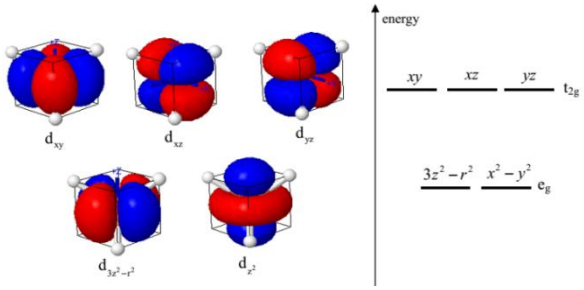

Fig. 1.10*:The orbitals of the octahedral field, the energy levels split into doubly degenerate e_g and triply degenerate t_{2g}. Unlike the tetrahedral field, the energy level of eg orbitals in octahedral field is higher than the energy level of t_{2g} orbitals (from reference [128]).*

Until this point, the contribution from covalent bonding in the transition metal cation-oxygen bond was not considered. The drawbacks of this assumption affect the crystal field splitting energy and provide an incomplete picture of the bonding. Although the bond is

mostly ionic, covalent bonding is also present. In fact, one limitation of crystal field theory is the improper prediction of the energy separation between the two orbital sets often referred to as the crystal field stabilization energy. Hence, the covalent bonding must be considered to provide a more precise separation energy value. For a cation residing in octahedral symmetry, its electronic configuration $(t_{2g})^m(e_g)^n$ is used to obtain the crystal field stabilization energy using the relation $\Delta(4m-6n)/10$. However, while the cation is in tetrahedral symmetry, its electronic configuration $(e_g)^p(t_{2g})^q$ is used to determine the crystal field stabilization energy using the formula $\Delta(6p-4q)/10$. In fact, it is found that the consideration of covalency improves the results.

Apart from the above theory, the molecular orbital theory can provide a more precise description of the bonding in these transition metal oxides[131]. This theory uses the concept of a delocalized electron approach in which it treats the bond between the transition metal cation and ligands as essentially covalent and also considers the effect of the orbital overlap.

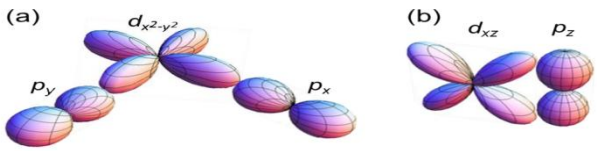

Figure.1.11: *(a) Schematic depicting the interaction between an e_g orbital and its ligands represented by the d_x^2-$_y^2$ and p_x and p_y orbitals. The direct overlap between these orbitals indicates strong interactions and σ bonding. (b) Schematic depicting the interaction between a t_{2g} orbital and a ligand represented by the d_{xz} and p_z orbitals. The indirect overlap between these orbitals results in weaker interactions and π bonding.*

In this approach, the ligands are not treated as the point charges and instead the shapes of the ligand bonding orbitals are considered. In fact, its illustration is easier for the octahedral field as its symmetry permits for easy depiction of the overlap. Fig. 1.11 (a) depicts the strong overlap between an antibonding e_g orbital and ligands represented by the $d_{x^2-y^2}$ and the p_x and p_y orbitals. The interaction between them becomes strongest as the lobes point directly at each other which is indicative of σ bonding. In contrast, Fig. 1.11 (b) demonstrates the indirect overlap between an antibonding t_{2g} orbital and ligand represented by the d_{xz} and p_z orbitals. This kind of overlap is indicative of π bonding.

On the other hand, the reduced symmetry of tetrahedral fields makes such an illustration much more complex. The antibonding t_{2g} orbitals form σ bonds with its ligands. However, bonds between the antibonding e_g orbitals and their ligands are a mixture of σ and π bonding as the π bonding is not independent of σ bonding.

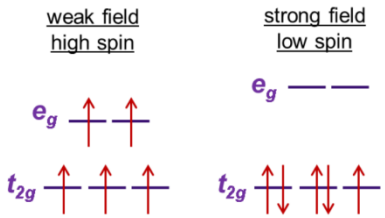

Figure. 1.12: *Schematic of the d orbital occupancy for a d^5 configuration with octahedral symmetry for the weak field and strong field cases.*

In such a system containing transition metal ions, the lowest energy spin configuration is achieved through the proper balance between the crystal field energy and Hund's energy which act to keep parallel alignment between spins. In fact, for a cation placed in octahedral co-ordination, the order in which orbital filling occurs is unambiguous for d^1 to d^3 systems and for d^8 to d^{10} configurations. Additionally, for all the other systems as well,

there is a potential for ambiguity associated with the order of orbital filling depending on the strength of the crystal field. At the extremes, as depicted in Fig. 1.12 for a d^5 octahedral configuration, a weak field (small crystal field energy) is synonymous with a high spin state in which spin-up electrons half-fill the lower energy orbitals then jump to and begin populating the higher energy orbitals maximizing the number of unpaired electrons. On the contrary, for a strong field (large crystal field energy), the competition between the crystal field and Hund's energies stabilizes a low spin state as an electron would prefer to pair up with the electrons in the lower lying, half-filled energy orbitals rather than incur the energy cost of overcoming the large crystal field energy in order to populate the higher energy orbitals. However, in between these extremes, there are systems in which the Hund's coupling and crystal field energy are closely competing and small external perturbations like temperature, pressure, and strain can push a system into high, low, or intermediate spin states. This phenomenon is known as the spin state transition and it has received tremendous research interest world-wide. The $RCoO_3$ (R=rare earth ions) type systems are well-known to exhibit such spin state transitions while at its ground state, the spin state of the Co^{3+} is known to remain in low-spin state.

1.3.2 Dzyaloshinsky-Moriya (D-M) interaction:

The Dzyaloshinsky-Moriya (D-M) interaction is also known as anisotropic exchange interaction which contributes towards the total magnetic exchange interactions between two neighboring spins [132]. In fact, in this special type of interactions, the spin-orbit interaction plays the major role in a similar manner that the oxygen ions play in the superexchange interactions between magnetic ions. In contrast to the exchange interactions where the excited state is connected via oxygen ions, in D-M interactions, the excited state is created by the spin-orbit interaction in one of the magnetic ions. An exchange interaction then occurs

between the excited state of one ion and the ground state of the other ion. When two spins S_1 and S_2 interact via D-M interactions, its Hamiltonian gets modified with an extra term expressed as:

$$\boldsymbol{H_{D-M} = \vec{D}.\overrightarrow{S_1} \times \overrightarrow{S_2}}$$

Here, $\vec{D}$ is a vector quantity which vanishes when the crystal field has "inversion symmetry" with respect to the centre of the two magnetic spins. However, in general this vector does not vanish and depending on the symmetry, it generally lies along the direction of the parallel or perpendicular to the line connecting the two spins. Eventually, the D-M interaction acts in such a way that it always tries to orient the two spins S_1 and S_2 at right angle with each other in a plane perpendicular to the direction of $\vec{D}$vector, thus ensuring the energy of the system to be negative. As a consequence, this interaction leads to the canting between the spins (by a small angle). Generally, D-M interactions occur in the antiferromagnetic systems and it raises an effective ferromagnetic moment due to spin canting along the perpendicular direction of the antiferromagnetic spin axis. It is often observed in the orthoferrite systems.

1.3.3 Spin-glass state:

The spin-glass state of a system referred to a magnetic state where the spins are not ordered and they are frozen in a random fashion at lower temperatures [132-138]. The term "glass" is related to the analogy of normal glasses where the atoms are randomly positioned and no periodicity is maintained unlike in the ordered crystals. In contrast to the ferromagnetic or anti-ferromagnetic materials where the spins are oriented in a fashion, in spin glass due to the competition between the ferromagnetic and anti-ferromagnetic interactions, the spins get frozen in a non-collinear random pattern. In fact, the rising magnetic frustration emanating from the competing magnetic interactions leads to the degenerate multivalley ground states, known as the spin glass. In such systems, the magnetic interactions among spins are in

conflict owing to the presence of the structural disorder (which is capable of pinning the spins) or geometrical spin frustration [133-135]. In pure FM or AFM systems, the domain formation involves microscopic time scales but due to the presence of disorder in a system, it causes pinning of the domain wall which essentially gives rise to metastable states which allow the domain walls to reach one state to other by thermally activated hopping. This process does not allow the system to attain an equilibrium state in the experimental time scale leading to a glassy magnetic phase which is manifested through the slow spin-relaxations, memory/aging effects, non-exponential decay, thermomagnetic irreversibility etc. Hence, presence of disorder plays a key role in triggering the glassy states in a system. On the other hand, in cluster glass (CG) state, the disorder or spin frustration occurs locally in small region of clusters [136-138]. The CG state evolves if one of the competing interactions (AFM or FM) is weaker relative to the other. The entity that is responsible for the cluster glass state is bigger than the atomic spins and they are the cluster of spins which can be treated as giant spin moment. However, the re-entrant spin or cluster glass state emerges when there is a long range magnetic ordering at higher temperature but it enters a glassy state at lower temperatures. Notwithstanding the complexity, re-entrant glassy state was nicely described by mean-field model as used by Sherrington- Kirkpatrick for Ising spin systems and the model introduced by Gabay and Toulouse for Heisenberg spin systems [139,140]. According to this model, long range order parameter still remains in the re-entrant glassy state.

1.3.4 Griffiths phase:

The Griffiths phase (GP) is a peculiar magnetic phase where the system neither behaves like a paramagnet nor shows long range ordering [141-155]. This phase evolves due to the nucleation of finite sized correlated regions or/and clusters having short range magnetic ordering embedded in the global paramagnetic matrix above magnetic transition temperature. In GP regime, the magnetization does not behave as an analytic function of the magnetic field

and it deviates from the Curie-Weiss law at temperatures much above the magnetic transition temperature. Eventually, though the experimental realization of GP was initially thought to be remote, Salamon et al was first to report an experimental observation of GP by magnetic susceptibility measurements on a hole doped manganite system. Hence, by measuring the temperature variation of the magnetic susceptibility at different fields, it is possible to probe the Griffiths like phase. "The temperature dependent inverse susceptibility curves i.e. χ^{-1} (T)" show a sharp down turn behaviour in the Griffiths phase regime which is considered to be a "hallmark" for identifying the Griffiths phase. It should be mentioned here that the observation of down-turn behaviour of χ^{-1} (T) at low fields is very crucial as it eventually helps one to distinguish the GP from other non-Griffiths like clustered phases where χ^{-1} (T) deviates from CW law by showing an up-turn above ordering temperature [143]. On increasing magnetic field, the down turn behaviour is observed to get softened and with sufficiently high field, it yields CW like behaviour, which is also a characteristic for GP. It is because of the fact that the magnetization increases linearly with magnetic fields in paramagnetic regions, thus at high fields, PM susceptibility dominates over the contribution from the correlated clusters to the susceptibility.

In 1969, in his original pioneering paper, Griffiths theoretically considered a percolation like problem in an Ising ferromagnet, where random dilution has been done by replacing the magnetic ions with non-magnetic ions or simply by creating vacancies [142]. Thus, the nearest neighbour with magnetic ions, the exchange bond strength is J occurring with a distribution probability p while the disorder introduced in the form of non-magnetic ions having bond strength 0 with the corresponding probability (1-p). In this scenario, the co-operative ferromagnetism cannot be established below a critical percolation threshold p_c of the associated lattice, since the theoretical probability for formation of infinite percolating "backbone" is zero (or divergence of correlation length is not possible). In case of p

exceeding threshold p_c, however, a relatively weak ferromagnetism is established due to shortage of percolation path but certainly at a temperature T_c^R below the long range FM ordering temperature of undiluted system T_G (=T_c^R @ p=1). The GP regime is thus defined by the temperature interval of $T_c^R(p)$< T< T_G, where singularities occur in the thermodynamic properties (e.g. magnetization) which become non-analytical function of fields, thus the system neither behaves like purely paramagnetic nor can attain long range FM order by forming infinite percolating chain. Later, Bray and Moore generalized this argument for any type of bond-distribution (not only bonds having strengths J and 0) formed due to disorder that eventually reduces the long range magnetic ordering temperature T_G to T_c, thus it greatly helped recognizing GP in various magnetic systems [141]. In GP regime, it doesn't follow CW law rather it follows the power law of inverse susceptibility with a characteristic non-universal exponent λ describing Griffiths singularity;

$$\chi^{-1}(T) \propto (T-T_c^R)^{1-\lambda}, (0<\lambda<1)$$

Here, the parameter λ is a measure of deviation from CW behaviour.

It is important to note here that initially a ferromagnetic system was thought to be a prerequisite for exhibition of Griffiths phase. However, recently, few reports have come up with the observation of Griffiths phase in some antiferromagnet as well and thus a paradigm shift has been observed [148-150]. Eventually, the susceptibility in the GP region involves both the paramagnetic susceptibility χ_{PM} and susceptibility due to magnetically ordered rare region χ_R. When the rare magnetic region (T <T_G) is FM, for low fields, χ_R dominates over χ_{PM}, thus results in down-turn behaviour of below $\chi^{-1}(T)$ below T_G. Albeit, if the rare region is AFM, the condition of χ_R>χ_{PM} may not always be satisfied, thus the down-turn behaviour which is the hall-mark of GP may not be observed. This is the reason why observation of GP is extremely rare in AFM systems.

1.3.5 Exchange bias effect:

Since its discovery in 1956 by Meiklejohn and Bean, the exchange bias effect has received intense research interest both theoretically and experimentally [156]. The discovery of exchange bias effect opened new frontier for the spintronic device applications viz., permanent magnets, read-heads, magnetic recording media, sensors, and many others. The exchange bias effect is manifested as a horizontal shift in magnetic the hysteresis loop. Eventually, the co-existence of multiple inhomogeneous magnetic phases in a system viz., FM/Spin glass, FM/Ferrimagnet, FM/AFM, hard/soft phases of FM systems etc often lead to the exhibition of the exchange bias (EB) [156-159]. Eventually, the exchange bias effect can be explained by the rise of a unidirectional and non-switchable anisotropy or the pinning force at the interface of the two different magnetic phases e.g. AFM/FM which causes the horizontal shift of the hysteresis loop by providing an additional remanence.

1.4 Motivation of the thesis

As compared to the widely studied pyrochlore compounds $A_2Ti_2O_7$ with A=Dy, Tb, Gd, Ho, Er and Yb, the europium titanate i.e.. $Eu_2Ti_2O_7$ system is relatively less studied system and hence there is much more opportunities to explore its magnetic properties. Nag (Chattopadhyay) et. al had showed that the $Eu_2Ti_2O_7$ system is a planar X-Y pyrochlore having crystal field effect driven strong single ion anisotropy effect [49]. A comprehensive study of the spin dynamics of this pyrochlore system is hitherto unreported; hence it can be interesting to investigate its ac susceptibility behaviours. Again, knowing the fact that the planar pyrochlore systems viz., $Er_2Ti_2O_7$, $Yb_2Ti_2O_7$ etc have received invigorated interest in recent past owing to their anisotropy driven novel exotic ground states, we have chosen the X-Y pyrochlore $Eu_2Ti_2O_7$ for exploring its spin dynamics.

On the other hand, the *4f-3d* interactions are well-known to produce interesting magnetic properties. Hence, we have incorporated Fe (*3d* element) in the Eu site to investigate the effect of *4f-3d* interactions in its magnetic properties as well as in its electronic properties. The comparable ionic radii of Ti^{4+} and Fe^{3+} are expected to raise the anionic disorder in the system which will alter its crystalline filed leading to a change in its single ion anisotropy. Thus, the incorporation of Fe has its potential to largely alter the spin dynamics of the system. Hence, we have made a detailed study of the electronic structure and spin dynamics of Fe substituted $Eu_2Ti_2O_7$ system.

Apart from the geometrically spin frustrated systems, we have also studied the site-disorder driven spin frustrated magnetism. We have chosen the fully B-site disordered double perovskite Pr_2CoFeO_6 system (or simply perovskite system $PrCo_{0.5}Fe_{0.5}O_3$) having orthorhombic structure in which at 4b site Co/Fe are randomly distributed. Since, both the Co and Fe ions are expected to be in similar trivalent oxidation states, it will give rise to the B-

site disordered structure. As it is already mentioned that B-site disorder has profound effects on the physical properties of the related systems, this provoked us to investigate the magnetic properties of such B-site disordered Pr_2CoFeO_6 system. Moreover, the electronic structure study of $PrCoO_3$ system has got renewed interest owing to its thermally assisted spin state transition. Hence, it is also interesting to study the effect of Fe substitution in Co site on its spin states.

As compared to the extensively studied partially or fully B-site ordered double perovskite compounds A_2BMnO_6 (A=La, Y, Lu, B=Co,Ni), the study on the Pr_2CoMnO_6 is very limited. In particular, its spin dynamics behaviour is not explored yet. Again, the hole doping in similar manganite systems has shown the evolution of many interesting properties viz, colossal magneto-resistance, giant exchange bias effect, magneto-caloric effects etc. Thus, we got motivated to study the electronic structure and the magnetization property measurements of hole doped partially disordered double perovskite $Pr_{2-x}Sr_xCoMnO_6$ (x=0.0, 0.3, 0.5) system.

References

1. C. Lacroix, P. Mendels, and F. Mila, Introduction to frustrated magnetism (Springer series in solid state sciences 164)
2. J. S. Gardner, M. J. P. Gingrasand J. E. Greedan, Rev. Mod. Phys. 82, 53 (2010) and the references therein.
3. Leon Balents , Nature 464, 199 (2010)
4. T. Taniguchi, H. Kadowaki, H. Takatsu, B. Fak, J. Ollivier, T. Yamazaki, T. J. Sato, H Yoshizawa , Y. Shimura and T. Sakakibara et al Phys. Rev. B 87, 060408 (2013)
5. J. S. Gardner, A. Keren, G. Ehlers, C. Stock, E. Segal, J. M. Roper, B. Fak, M. B. Stone, P. R. Hammar, and D. H. Reich et al Phys. Rev. B 68, 180401(R) (2013)
6. G. Ehlers, J.E. Greedan, J. R. Stewart, K. C. Rule, P. Fouquet, A. L. Cornelius, C. Adriano , G. Pagliuso, Y. Qiu and J. S. Gardner Phys. Rev. B 81, 224405 (2010)
7. D. K. Singh, Y. S. Lee, Phys. Rev. Lett. 109, 247201 (2012)
8. S. Iguchi, Y. Kumano, K. Ueda, S. Kumakura and Y. Tokura, Phys. Rev. B 84, 174416 (2011)
9. A. P. Ramirez, A. Hayashi, R. J. Cava, R. Siddharthan and B. S. Shastry, Nature 399, 333 (1999)
10. J. Snyder, B.G. Ueland , J. S. Slusky, H. Karunadasa, R. J. Cava, and P. Schiffer, Phys. Rev. B 69, 064414 (2004)
11. J. Snyder, J. S. Slusky, R. J. Cava, and P. Schiffer, Nature 413, 48 (2001)
12. J. Oitmaa, R. R. P. Singh , B. Javanparast, A. G. R. Day, B. V. Bagheri, and M. J. P. Gingras, Phys Rev B 88, 220404 (2013)
13. L. Savary, K. A. Ross, B. D. Gaulin, J. P. C. Ruff and L. Balents, Phys Rev Lett, 109, 1672201 (2012)
14. J. D. M. Champion, M. J. Haris, P. C. W. Holdsworth, A. S. Wills, G. Balakrishnan, S. T. Bramwell, E. Cizmar, T. Fennell, J. S. Gardner and J. Lago et. al. Phys. Rev. B 68, 020401(R) (2003)
15. N. P. Raju, et. al., Phys. Rev. B. 59, 14489 (1999)
16. J. D. M. Champion et. al. Phys. Rev. B, 64, 140407 (2001)

17. K.E. Sickafus, L. Minervini, R.W. Grimes, J.A. Valdez, M. Ishimaru, F. Li, K.J. McClellan, T. Hartmann, Science 289, 748 (2000).
18. J. Lian, J. Chen, L.M. Wang, R.C. Ewing, Phys. Rev. B 64, 134107 (2003).
19. M. A. Subramanian, and A. W. Sleight, 1993, Handbook on the Physics and Chemistry of Rare Earths, (Elsevier Science, New York, p.225.)
20. I. O. Troyanchuk, Inorg. Mater. 26, 182. (1990)
21. G. Ehlers, A. L. Cornelius , M. Orendac, M. Kajnakova, T. Fennell, S. T. Bramwell and J. S. Gardner, J. Phys. : Cond. Matt. 15, L-9 (2003)
22. J. Snyder et. al. Phys. Rev. B 66, 064432 (2002)
23. J. Snyder et. al., Phys. Rev. Lett. 91, 107201 (2003)
24. A. P. Ramirez, A. Hayashi, R. J. Cava, R. Siddharthan, B. S. Shastry, Nature, 399, 333 (1999)
25. L. D. C. Jaubert, P. C. Holdsworth, Nat. Phys.5, 258 (2009)
26. I. Mirebeau, I. N. Goncharenko, P. Cadavez-Peres, S. T. Bramwell, M. J. P. Gingras, and J. S. Gardner, Nature (London) 420, 54 (2002).
27. B. G. Uelandet. al., Phys. Rev. Lett. 96, 027216 (2006)
28. M. Mączka, et. al. Phys. Rev. B 78, 134420 (2008)
29. S. T. Bramwellet. al., Phys. Rev. Lett. 87, 047205 (2001
30. A. L. Cornelius et. al., Phys. Rev. B 64, 060406 (2001)
31. K Matsuhiraet. al., J. Phys.: Condens. Matter 12,L649 (2000)
32. G Ehlers et. al., J. Phys.: Condens. Matter 16,S635 (2004)
33. Moessner, R., and J. T. Chalker, Phys. Rev. B 58, 12049 (1998a)
34. Moessner, R., and J. T. Chalker, Phys. Rev. Lett. 80, 2929 (1998b)
35. Canals, B., and C. Lacroix, Phys. Rev. Lett. 80, 2933 (1998)
36. Canals, B., and C. Lacroix, Phys. Rev. B 61, 1149 (2000)
37. S. E. Palmer, and J. T. Chalker, Phys. Rev. B 62, 488 (2000)
38. P. Bonville, et. al., J. Phys.: Condens. Matter 15, 7777 (2003)
39. A. P. Ramirez et. al., Phys. Rev. Lett 89, 067202 (2002)
40. M. E. Zhitomirskyet. al., Phys. Rev. Lett. 109, 077204 (2012)
41. J. P. C. Ruff et. al., Phys. Rev. Lett. 101, 147205 (2008)
42. M. E. Zhitomirskyet. al., Phys. Rev. B 89, 140403(R) (2014)
43. P. Dalmas de R´eotier, et. al., Phys. Rev. B 86, 104424 (2012)
44. M. Orenda´cet. al., Phys. Rev. B 93, 024410 (2016)

45. L. J. Chang et al. Nat. Commun. 3:992 (2012).
46. R. M. D'Ortenzioet. al., Phys. Rev. B 88, 134428 (2013)
47. J. S. Gardner et. al., Phys. Rev. B 70, 180404(R) (2004)
48. C. Mauwset. al., Phys. Rev. B 98, 100401(R) (2018)
49. A. Nag (Chattopadhyay), P. Dasgupta, Y.M. Jana, D. Ghosh, J. Ally. Comp. 384, 6 (2004).
50. P. Dasgupta, Y.M. Jana, A.N. Chattopadhyay, R. Higashinaka, Y. Maeno, D. Ghosh, J. Phys. Chem. Solid. 68 (2007) 347.
51. G.R. Haripriya, H.S. Nair, R. Pradheesh, S. Rayaprol, V. Siruguri, D. Singh, R. Venkatesh, V. Ganesan, K. Sethupathi, and V. Sankaranarayanan, J. Phys.: Condens. Matter. 29, 475804 (2017).
52. N.S. Rogado, J. Li, A.W. Sleight, and M.A. Subramanian, Advanced Materials 17, 2225 (2005).
53. J. Blasco, J. García, G. Subías, J. Stankiewicz, J.A. Rodríguez-Velamazán, C. Ritter, J.L. García-Muñoz, and F. Fauth, Phys. Rev. B 93, 214401 (2016).
54. D. Choudhury, P. Mandal, R. Mathieu, A. Hazarika, S. Rajan, A. Sundaresan, U.V. Waghmare, R. Knut, O. Karis, P. Nordblad, and D. D. Sarma, Phys. Rev. Lett 108, 127201 (2012).
55. H.S. Nair, D. Swain, H. N., S. Adiga, C. Narayana, and S. Elzabeth, J. App. Phys. 110, 123919 (2011).
56. T. Chakraborty, H. S. Nair, H. Nhalil, K. R. Kumar, A. M. Strydom and S. Elizabeth, J. Phys. Cond. Mater. 29, 025804 (2017).
57. R. I. Dass and J. B. Goodenough, Phys. Rev B 67, 014401 (2003).
58. M. G. Hernández, J. L. Martínez, M. J. M. Lope, M.T. Casais and J. A. Alonso, Phys. Rev. Lett. 86, 2443 (2001).
59. A. S. Ogale, S. B. Ogale, R. Ramesh, and T. Venkatesan, App. Phys. Lett. 75, 537 (1999).
60. G. Sharma, J. Saha, S. D. Kaushik, V. Siruguri, and S. Patnaik, App. Phys. Lett. 103,012903 (2013).
61. L. Shlyk, S. Strobel, B. Farmer, L. E. De Long,2, and R. Niewa, Phys. ReV. B 97, 054426 (2018)
62. A. K. Pramanik and A. Banerjee, Phys. Rev. B 81, 024431 (2010) (GP PSMO)
63. J. B. Goodenough, Phys. Rev. 100, 564 (1955).

64. K. D. Truong, M. P. Singh, S. Jandl, and P. Fournier, Phys. Rev. B 80, 134424 (2009) and references therein.
65. M. P. Singh, K. D. Truong, S. Jandl, and P. Fournier, Phys. Rev. B 79, 224421 (2009)
66. S. Baidya and T. Saha-Dasgupta, Phys. Rev. B 84, 035131 (2011)
67. M. K. Kim et. al., J. Phys.: Condens. Matter 27 (2015) 426002 (6pp)
68. J. Krishna Murthy and A. Venimadhav, J. App. Phys 113, 163906 (2013)
69. J. Krishna Murthy and A. Venimadhav, J. App. Phys. 111, 024102 (2012)
70. M. Zhu et. al., App. Phys. Lett. 100, 062406 (2012)
71. Y. Mao, Nanoscale. 5, 4720 (2013)
72. M. Ullah, et. al., J. Magn. Magn. Mater. 377, 197 (2015)
73. J.K. murthy,A.Venimadhav, AIP Conf. Proc.1447 (2012)1235.
74. M. Bejaret. al., J. Ally. Comp. 440, 36 (2007)
75. Ch. Meyer et. al., Phys. Rev. B 98, 134433 (2018)
76. R. N. Mahato, J. App. Phys. 107, 09D714 (2010)
77. J. Krishna Murthy and A. Venimadhav, App. Phys. Lett. 103, 252410 (2013)
78. Y. Guoet. al., J. Phys. D: Appl. Phys. 46,175302 (6pp) (2013)
79. Y. Guoet. al., App. Phys. Lett. 102, 222401 (2013)
80. R. Takahashi, et. al, Phys. Rev. B 91, 134107 (2015)
81. J. Krishna Murthy et. al.,Euro. Phys. Lett., 108, 27013 (2014)
82. H. S. Nair et. al., J. App. Phys. 116, 123907 (2014)
83. H. S. Nair et. al., App. Phys. Lett. 106, 022407 (2015)
84. G. Sharma et. al., Applied Physics Letters 103, 012903 (2013)
85. J. Krishna Murthy and A. Venimadhav, J. Phys. D: Appl. Phys. 47, 445002 (6pp) (2014)
86. S. Kumar et. al., Phys. Rev. B 82, 134429 (2010)
87. R. B. M. Filho, App. Phys. Lett. 102, 192902 (2013)
88. J. Su et. al., ACS Appl. Mater. Interfaces, 7, 13260(2015)
89. R. P. Maiti, J. App. Phys. 112, 044311 (2012)
90. H. Nhalilet. al., Phys. Rev. B 92, 214426 (2015)
91. S. Y-Vilaret. al., Phys. Rev. B 84, 134427 (2011)
92. N. Lee, Appl. Phys. Lett. 104, 112907 (2014)
93. H. Y. Zhou et. al., Appl. Phys. Lett. 106, 152901 (2015)

94. J. T. Zhang et. al., Phys. Rev. B 93, 075140 (2016)
95. S. Chandaet. al., J. Appl. Phys. 120, 134102 (2016)
96. L. Zhang et. al., J. Ally Comp 763, 613e621 (2018)
97. W. Liu et. al., J. App. Phys. 116, 193901 (2014)
98. M. P. Singh et. al., Appl. Phys. Lett. 98, 162506 (2011)
99. K. D. Truong et. al., J. Phys.: Condens. Matter 23, 052202 (5pp) (2011)
100. C. Ganeshraj, R. Pradheesh, P. N. Santhosh, J. Appl. Phys. 111, 07A914 (2012)
101. Md G. Masud, J. Appl. Phys. 118, 064104 (2015)
102. L. Wang et. al., J. Appl. Phys. 117, 17D914 (2015)
103. S. K. Giriet. al., J. Phys. D: Appl. Phys. 49, 165002 (7pp) (2016)
104. W. Z. Yang et. al.,J. Appl. Phys. 112, 064104 (2012)
105. P. NeenuLekshmiet. al., J. Mater. Chem. C, 1, 6565 (2013)
106. A.Rathiet. al., J. Phys. D: Appl. Phys. 50,465001 (5pp) (2017)
107. A. Anshulet. al., J. Appl. Phys. 115, 084106 (2014)
108. R. R. Das et. al., J. Ally. Comp 773,770e777 (2019)
109. C. Xieet. al., J. Appl. Phys. 120, 155302 (2016)
110. R. Yadavet. al.,J. Appl. Phys. 117, 053902 (2015)
111. A. K. Singh et. al., Solid State Commun. 242, 74 (2016)
112. C. Shi, J. Phys. D: Appl. Phys. 44, 245405 (6pp) (2011)
113. A. K. Singh et. al., Appl. Phys. Lett. 110, 102402 (2017)
114. X.L. Wang et. al, Solid State Communications 118, 27 (2001)
115. J. Y. Moon et. al., Sci. Rep, 7, 16099 (2017)
116. J Krishna Murthy et. al., J. Phys. D: Appl. Phys. 48,355001 (6pp) (2015)
117. J. Krishna Murthy et. al., J. Ally Comp 719,341e346 (2017)
118. R. C. Sahooet. al.,J. Appl. Phys. 124, 103901 (2018)
119. R. X. Silva et. al., J. Appl. Phys. 114, 194102 (2013)
120. S. H. Oh et. al.,J. Phys. D: Appl. Phys. 48, 445001 (5pp) (2015)
121. R. B. MacedoFilhoet. al., Mater. Res. Express 2, 075201 (2015)
122. V A Khomchenkoet. al., J. Phys.: Condens. Matter 18, 9541 (2006)
123. J. Y. Moon et. al., Phys. Rev. B 98, 174424 (2018)
124. T. Chatterjeeet. al., J. Phys.: Condens. Matter 24, 266005 (7pp) (2012)
125. H. S. Nair et. al., J. Appl. Phys. 110, 123919 (2011)

126. A. Banerjee et. al., Phys. Rev. B 98, 104414 (2018)
127. M. K. Kim et. al., Sci. Rep. 9: 5456 (2019)
128. R. J. Lancashire, CHEM1902 (C10K) Co-ordination Chemistry, An introductory course at UWI, Jamaica. 2010
129. J. D. Dunitz and L. E. Orgel; J.Phys. Chem. Solids, 3, 318 (1957)
130. C. J. Ballhausen and J. Dan, Mat. Fys. Medd, 29, 4 (1954)
131. F. A. Cotton, Chemical applications of group theory, Wiey, Newyork, 1990
132. S. Blundell, Magnetism in condensed matter, Oxford master series in condensed matter physics, Oxford University press Inc, New York (2001).
133. J. Knolle, G.-W. Chern, D. L. Kovrizhin, R. Moessner, and N. B. Perkins, Phys. Rev. Lett. 113, 187201 (2014).
134. J. A. Mydosh, Spin Glass: An Experimental Introduction (Taylor and Francis, London, 1993).
135. K. Binder and A. P. Young, Rev. Mod. Phys. 58, 801 (1986).
136. C. Djurberg, P. Svedlindh, P. Nordblad, M. F. Hansen, F. Bødker, and S. Mørup, Phys. Rev. Lett. 79, 5154 (1997).
137. A. Ito, H. Aruga, E. Torikai, M. Kikuchi, Y. Syono, and H. Takei, Phys. Rev. Lett. 57, 483 (1986).
138. M. D. Mukadam, S. M. Yusuf, P. Sharma, S. K. Kulshreshtha, and G. K. Dey, Phys. Rev. B 72, 174408 (2005) and references therein.
139. D. Sherrington and S. Kirkpatrick, Phys. Rev. Lett. **32**, 1782 (1975).
140. M. Gabay and G. Toulouse, Phys. Rev. Lett. 47, 201 (1981).
141. A. J. Bray, M. A. Moore, J. Phys. C **15**, L765 (1982).
142. R. B. Griffiths, Phys. Rev. Lett. **23**, 17 (1969)
143. C. He, M. A. Torija, J. Wu, J. W. Lynn, H. Zheng, J. F. Mitchell, C. Leighton, Phys. Rev. B **76**, 014401 (2007).
144. M. B. Salamon, P. Lin, and S. H. Chun, Phys. Rev. Lett. **88**, 197203 (2002).
145. A.H.C. Neto, G. Castilla, and B.A. Jones, Phys. Rev. Lett. **81**, 3531 (1998)
146. A. K. Pramanik and A. Banerjee, Phys. Rev. B **81**, 024431 (2010)
147. Z.W. Ouyang, N.M. Xia, Y.Y. Wu, S.S. Sheng, J. Chen, Z.C. Xia, L. Li, and G.H. Rao, Phys. Rev. B **84**, 054435 (2011).
148. A Karmakar, S Majumdar, S Kundu, T K Nath and S Giri, J. Phys.: Condens. Matter **25**, 066006 (2013).

149. K. Ghosh, C. Mazumdar, R. Ranganathan, S. Mukherjee, Sci. Rep. **5**, 15801 (2015).

150. J. Kumar, S. N. Panja, S. Dengre, S. Nair, Phys. Rev. B **95**, 054401 (2017)

151. A. J. Bray, Phys. Rev. Lett. **60**, 720 (1988).

152. M. Randeria, J. P. Sethna, and R. G. Palmer, Phys. Rev. Lett. **54**, 1321 (1985).

153. J. Fan, L. Pi, Y. He, L. Ling, J. Dai, and Y. Zhang, J. App. Phys. **101**, 123910 (2007).

154. Y. Imry and S. K. Ma, Phys. Rev. Lett. **35**, 1399 (1975).

155. J. Deisenhofer, D. Braak, H.-A. Krug von Nidda, J. Hemberger,R. M. Eremina, V. A. Ivanshin, A. M. Balbashov, G. Jug, A.Loidl, T. Kimura, and Y. Tokura, Phys. Rev. Lett. **95**, 257202 (2005).

156. W. H. Meiklejohn and C. P. Bean, Phys. Rev. **102**, 1413 (1956).

157. M. Ali, P. Adie, C.H. Marrows, D. Greig, B.J. Hickey, and R.L. Stamps, Nat. Mater. 6, **70** (2006).

158. Q. K. Ong, A. Wei, and X.M. Lin, Phys. Rev. B **80**, 134418 (2009).

159. B.M. Wang, Y. Liu, P. Ren, B. Xia, K.B. Ruan, J.B. Yi, J. Ding, X.G. Li, and L. Wang, Phys. Rev. Lett. **106**, 077203 (2011).